High mobility group protein AT-hook 1 (HMGA1) is a nuclear matrix protein with three AT-hook domains that bind the minor groove of AT-rich DNA sequences [2,3]. HMGA1 modulates the activity of many transcription factors by inducing a conformational change in DNA via AT-rich DNA sequence binding [2]. HMGA1 also modulates the molecular or cellular function of other molecules, including p53 [4] and Rb [5], via protein–protein interactions. HMGA1 is highly expressed during embryogenesis, but is not expressed or expressed at very low levels in normal differentiated adult tissues [6]. HMGA1 is overexpressed in cancers of various tissues [7]. The increased expression of HMGA1 in PCa has been reported both in surgical specimen and cell lines. The expression of HMGA1 is associated with high grade and metastatic potential in human PCa [8,9]. HMGA1 expression is low in the androgen-responsive metastatic PCa cell line (LNCaP), but is high in the androgen-independent metastatic PCa cell line (PC-3, DU145) [10]. We previously reported that the level of HMGA1 expression in PCa cells is correlated with the extent of chromosomal aberrations [10] and that transfecting HMGA1 into PCa cell lines induces unbalanced chromosomal rearrangement [10] and expression of matrix metalloproteinase 2 [11]. We also have reported that HMGA1 expression in the transgenic adenocarcinoma of the mouse prostate (TRAMP) model was confined to the later stage when metastatic lesions formed [12]. These findings suggest that HMGA1 is a strong candidate gene playing a potential role in the progression of PCa. These previously reported findings prompted us to examine if HMGA1 is associated with developing androgen-independence, which is one of important biological features obtained by lethal phenotype of PCa during progression.

The purpose of this study is to determine how HMGA1 is associated with the progression of androgen-dependent PCa cells into androgen-independent cancer cells as well as with the proliferation of androgen-independent PCa cells.

MATERIALS AND METHODS

Cell Culture and Transfection

LNCaP is androgen-responsive human PCa cell line. DU145 and PC-3 are androgen-independent human PCa cell lines. LNCaP, DU145, and PC-3 cells were maintained in RPMI1640 containing 10% fetal bovine serum (FBS). LN95 cells were kindly provided by Dr. Alan Meeker (Johns Hopkins University, Baltimore, MD). The androgen-dependent LNCaP cell line was induced to an androgen-independent subline (LN95) by being maintained for long periods of time in the absence of androgens [13]. LN95 cells were maintained in RPMI1640 (Phenol red-free) containing 10% charcoal-dextran treated FBS (CDS). LNCaP cells were transfected with plasmids expressing mouse HMGA1a and pBABE-puro for puromycin resistance as previously described [10]. Transfected cells were maintained in medium containing puromycin (0.60 μg/ml). LNCaP cell transfected with HMGA1a vector (LN-H1) and LNCaP cell transfected with control empty vector (LN-EV) were established by one of the authors at Dr. Donald S. Coffey's laboratory (Johns Hopkins University, Baltimore, MD) [10] and then were taken over and kept by Dr. Robert H Getzenberg (Johns Hopkins University, Baltimore, MD). These transfected LNCaP cells were kindly provided for us by Dr. Robert H Getzenberg.

Cell Proliferation Assay

LN-H1 cells and LN-EV cells were seeded in replicates of 6 into 96-well plates at a density of 5,000 cells/well in RPMI1640 (Phenol red-free) containing 10% CDS. On the second day and 6th day, cells were supplemented with 0–1 nM dihydrotestosterone (DHT) dissolved in ethanol (final ethanol concentration was 0.001%). DU145 and PC-3 cells were seeded in replicates of 6 into 96-well plates at a density of 5,000 cells/well using RPMI1640 containing 10% CDS and the transfection of siRNAs was performed on the following day. Cell proliferation of DU145 and PC-3 was estimated in RPMI1640 containing 10% CDS. Cell proliferation was estimated using Cell counting kit-8 (WST-8) (Dojindo) according to the manufacturer's instructions.

Small Interfering RNA-Mediated Knockdown

Synthetic double-stranded small interfering RNAs (siRNA) were transfected at a concentration of 200 nM using Oligofectamine (Invitrogen) according to the manufacturer's instructions. The siRNAs with the following sequences (target sequence, sense strand) were used: scramble (control) siRNA 5′-CAGTCGCGTTTGCGACTGGdTdT-3′, HMGA1 siRNA 5′-GACCCGGAAAACCACCACAdTdT-3′ [14]. These siRNAs were purchased from Sigma.

Protein Preparation

Whole cell lysate (WCL) was prepared from each cell line and each tissue sample in RIPA Lysis Buffer (Santa Cruz Biotechnology) as described by the manufacturer. Nuclear extracts (NE) were prepared from each cell line by Nuclear Extract Kit (Active Motif) as

described by the manufacturer. Protein concentration was measured using BCA Protein Assay Kit (Pierce).

Western Blot Analysis

Protein samples were separated in 15% polyacrylamide gel (Bio-Rad) and transferred to a nitrocellulose membrane (GE Healthcare). The membrane was probed with anti-HMGI (Y) antibody (N19; Santa Cruz Biotechnology) at a dilution of 1:200 and then with anti-goat IgG-HRP antibody (R&D Systems) at a dilution of 1:3,000. The signal was detected with an enhanced chemiluminescence kit (GE Healthcare) [10,11]. The membrane was probed with anti-AR antibody (N20; Santa Cruz Biotechnology) at a dilution of 1:1,000 and then with anti-rabbit IgG-HRP antibody (Jackson ImmunoResearch) at a dilution of 1:10,000. The monoclonal antibody against β-actin (clone AC15; Sigma) at a dilution of 1:5,000, and the antibody against Sp1 (Sigma) at a dilution of 1:400 were used to control sample loading of WCL and NE, respectively. The signal of AR, β-actin, and Sp1 was detected with a chemiluminescence kit (GE Healthcare).

In Vivo Experiment

Fourteen-week-old BALB/c male mice underwent surgical castration or sham operation (n = 7 for each group). The mice were sacrificed and their prostate tissues were collected 4 and 11 days after the operation.

LNCaP cells (5×10^6 cells in 0.1 ml RPMI1640 containing 10% FBS) suspended in an equal volume of Matrigel (Becton Dickinson) were injected subcutaneously in the flank region of 10-week-old male nude mice (BALB/c-nu/nu). The tumor formation ability of the cells was assessed by the tumor volumes. Tumor volumes were measured once a week and their volumes were calculated using the formula: volume = 0.532 × length × width × height. Castration and sham operation were performed at the time when the tumor volume was 88 mm^3 in average (n = 7 for each group). Eight days after the operations, the mice were sacrificed and the formed tumors were collected. All the animal experiments were approved by institutional animal care committee.

Statistical Analysis

Multiple independent experiments were performed for each set of data presented, and the results are presented as the mean ± SD. Student's *t*-test was used to identify significant differences between the control and experimental groups. Differences were considered statistically significant at $P < 0.05$.

RESULTS

The HMGAI Expression Was Higher in Androgen-Independent Prostate Cancer Cells Than in Androgen-Dependent Prostate Cancer Cells

We have previously reported that the levels of HMGA1 protein were higher in DU145 and PC-3 cells than in LNCaP cells [10]. Similarly in this study, Western blot analysis indicated that the HMGA1 protein expression in WCL from androgen receptor (AR)-negative PCa cell lines, DU145 and PC-3, was 1.6- and 3.1-fold higher than that from AR-positive PCa cell line, LNCaP, respectively (Fig. 1A). LN95 cell is an androgen-independent AR-positive subline of LNCaP established by maintaining them for long period in the absence of androgens. The expression of HMGA1 in NE from LN95 cells assessed by Western blot analysis was 2.5-fold higher than that in the parental LNCaP cells (Fig. 1B). The HMGA1 expression in androgen-independent PCa cells was higher than that in androgen-dependent PCa cells regardless of the expression status of AR.

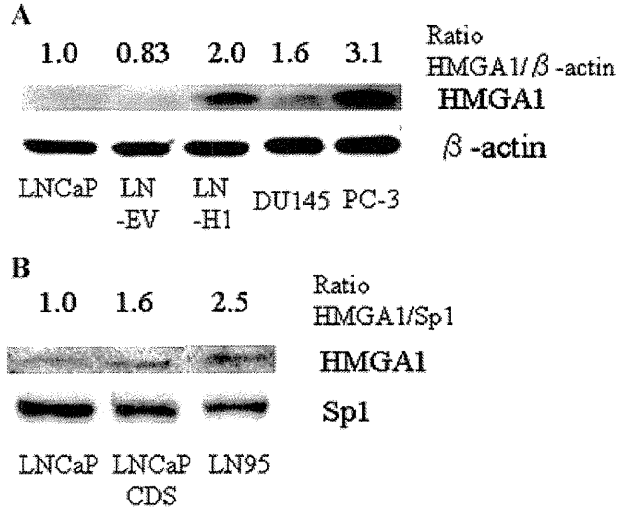

Fig. 1. HMGAI expression in androgen-dependent and -independent prostate cancer cells. **A**: Expression of HMGAI and β-actin (loading control) in whole cell lysate proteins of LNCaP, DUI45, PC-3, LN-HI (LNCaP cells transfected with HMGAI), and LN-EV (LNCaP cells transfected with control empty vector) cells was examined by Western blot analysis. **B**: Expression of HMGAI and Spl (loading control) in nuclear extract proteins of LNCaP and LN95 cells was examined by Western blot analysis. Androgen-deprivation induced an increase in the level of HMGAI in LNCaP cells. LN95: androgen-independent subline of LNCaP by being maintained for long time in the absence of androgens, LNCaP CDS: protein sample was extracted 4 days after growing the parental LNCaP in RPMIl640 medium containing l0% charcoal-dextran treated FBS (CDS).

Androgen-Deprivation Induced an Increase in the Level of HMGAI in LNCaP Cells

Increased expression of HMGA1 in LN95 suggests that long term androgen-deprivation might have induced an increase in the level of HMGA1 in LNCaP cells. To evaluate if short term androgen-deprivation can also induce the expression of HMGA1, the expression level of HMGA1 protein in NE from LNCaP cells was examined by Western blot analysis after LNCaP cells were cultured under androgen-deprived conditions (RPMI 1640 with 10% CDS) for 4 days. Androgen-deprivation for 4 days induced a 1.6-fold increase in the level of HMGA1 in parental LNCaP cells (Fig. 1B). Short-term as well as long-term androgen-deprivation induced an increase in the level of HMGA1 protein in LNCaP cells.

Androgen-Deprivation Induced an Increase in the Level of HMGAI in LNCaP Xenograft Model In Vivo

To examine if the expression of HMGA1 is induced by androgen-deprivation not only in vitro but also in vivo, LNCaP xenograft model was studied. LNCaP cells were injected subcutaneously and the tumors were formed in nude mice. After the LNCaP tumors were formed, one group of mice underwent surgical castration, and the other group underwent sham operations, and then tumor tissue of each mouse was collected 8 days after the operations. Western blot analysis demonstrated that the expression of HMGA1 protein was almost undetectable in the WCL extracted from LNCaP tumors of sham operation group while the expression of HMGA1 protein was detected in LNCaP tumors of castration group (Fig. 2). Androgen-deprivation induced the expression of HMGA1 protein in androgen-dependent LNCaP not only in vitro but also in vivo.

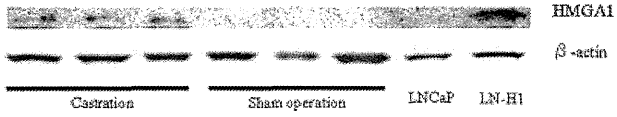

Fig. 2. Induction of HMGAI in LNCaP xenograft model in vivo by androgen-deprivation. Expression of HMGAI and β-actin (loading control) in whole cell lysate proteins of LNCaP tumor was examined by Western blot analysis. LNCaP cells were injected subcutaneously in male nude mice. The mice were randomly divided into two groups; one group underwent surgical castration, and the other group underwent sham operation (n = 7 for each group). Eight days after operation, the animals were sacrificed and tumor tissues were collected. HMGAI was expressed in tumor tissues from the castrated mice, but not in tumor tissues from the sham-operated mice. Whole cell lysate protein sample of LN-HI cells was a positive control.

Androgen-Deprivation Did Not Induce an Increase in the Level of HMGAI in Normal Adult Prostate Tissue

To determine if androgen-deprivation induces expression of HMGA1 not only in PCa but also in the normal adult prostate, the following mouse experiment was performed. One group of mice underwent surgical castration, and the other group underwent sham operations, and the prostate tissues of each group of mice were collected 4 and 11 days after the operations. Western blot analysis demonstrated that the expression of HMGA1 protein was almost undetectable in WCL extracted from normal prostate tissues of adult mice 4 days after castration as well as that of adult mice 4 days after sham operation (Fig. 3A). Quantitative RT-PCR also indicated that the mRNA expression level of HMGA1 in normal prostate tissues of adult mice 4 days after castration was almost same with that of adult mice 4 days after sham operation (data not shown). Similarly, the expression of HMGA1 in the normal prostate of adult mice 11 days after castration as well as that of sham operation was demonstrated to be very low and almost undetectable by Western blot analysis (Fig. 3B). It is suggested that significant level of HMGA1 expression is not induced by androgen-deprivation in normal adult prostate tissue.

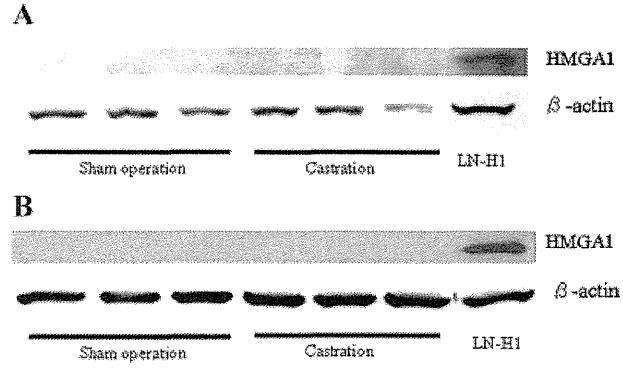

Fig. 3. No detectable induction of HMGAI in normal adult mouse prostate tissue by androgen-deprivation. Expression of HMGAI and β-actin (loading control) in whole cell lysate proteins of adult mouse prostate tissue was examined by Western blot analysis. The mice were randomly divided into two groups; one group underwent surgical castration, and the other group underwent sham operation (n = 7 for each group). **A**: Western blot of whole cell lysate protein of normal prostate tissues 4 days after operation. **B**: Western blot of whole cell lysate protein in normal prostate tissues 11 days after operation. The HMGAI level in normal prostate tissue from adult mice at 4 or 11 days after castration was very low and similar to that in the sham-operated mice. Whole cell lysate protein sample of LN-HI cells was a positive control.

Overexpression of HMGAI Attenuated the Suppression of Cell Proliferation of LNCaP Under Androgen-Deprived Condition

It was suggested that short-term androgen-deprivation induces an increase in the level of HMGA1 in the androgen-dependent parental LNCaP cells and long-term androgen-deprivation resulted into increased expression of HMGA1 in androgen-independent LNCaP subline LN95 cells, respectively (Fig. 1B). Therefore, we evaluated the effect of overexpressed HMGA1 on cell proliferation of LNCaP cells under the conditions of various concentrations of androgen. The cell proliferation rates of LNCaP cell transfected with HMGA1a vector (LN-H1) and LNCaP cell transfected with control empty vector (LN-EV) were examined by WST-8 assay. The expression of HMGA1 protein in WCL and NE from LN-H1 was confirmed to be 2.4- and 3.2-fold as high as that of LN-EV, respectively (Figs. 1A and 4A). This finding is similar to that in our previous report [10]. The cell proliferation curves of LN-EV and LN-H1 are compared in Figure 4B. LN-EV and LN-H1 grew equally well in control medium containing 10% FBS. In addition, both LN-EV and LN-H1 grew better in control medium than in androgen-deprived medium containing 10% CDS with 0–1 nM DHT. The cell proliferation rate at day 8 of LN-H1 grown in low concentration (0–0.01 nM) of DHT was about twofold higher than that of LN-EV. LN-EV cell could not keep proliferation over day 6, while LN-H1 could maintain proliferation over day 6. In contrast, both LN-H1 and LN-EV cells grew equally well in higher concentrations (0.1–1 nM) of DHT and could also keep proliferation over day 6. It is suggested that the overexpression of HMGA1 might attenuate the suppression of cell proliferation of LNCaP under androgen-deprived condition.

Since the cell proliferation rate of LN-H1 was demonstrated to be higher than that of LN-EV grown in low concentration (0–0.01 nM) of DHT, we evaluated the expression level of AR in LN-EV and LN-H1 cells by Western blot analysis. The protein level of AR in LN-H1 cells was almost same with that of LN-EV cells (Fig. 4C). The band of about 75 kDa, which appears to be AR spliced variant, was detected in LN95 cells, but not in both LN-EV cells and LN-H1 cells.

Knockdown of HMGAI Suppressed DU145 and PC-3 Cell Proliferation in Androgen-Deprived Condition

To elucidate the role of HMGA1 in cell proliferation of androgen-independent PCa cells, we used RNA interference. Knockdown of HMGA1 protein was observed in DU145 cells and PC-3 cells 2 days after the transfection of the HMGA1 siRNA. The

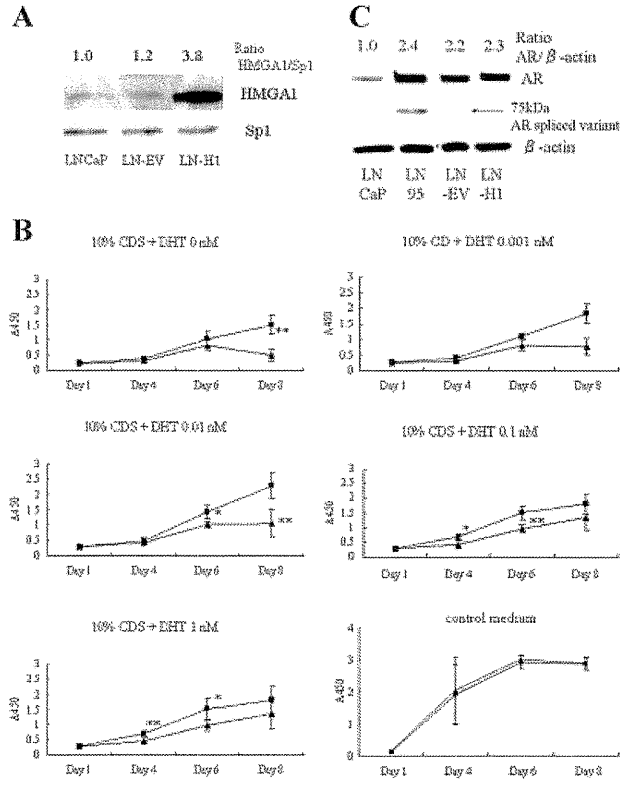

Fig. 4. Overexpression of HMGAI attenuated the suppression of cell proliferation of LNCaP under androgen-deprived condition. **A**: Expression of HMGAI and SpI (loading control) in nuclear extract proteins of LNCaP, LN-HI (LNCaP transfected with HMGAI), and LN-EV (LNCaP transfected with control empty vector) cells, was examined by Western blot analysis. **B**: Cell growth curves for LN-EV (▲) and LN-HI (■) cells. LN-EV and LN-HI cells were seeded in control medium or RPMII640 (Phenol red-free) containing 10% charcoal-dextran treated FBS (CDS). On day 2 and 6, cells were treated with 0–I nM dihydrotestosterone (DHT). The cell proliferation rate at day 8 of LN-HI grown in low DHT concentrations (0–0.0I nM) was about twofold that of LN-EV. In contrast, both LN-HI and LN-EV cells grew equally well in high DHT concentrations (0.I–I nM), and in control medium. Value are means ± SD. $^{*}P < 0.05$; $^{**}P < 0.00I$ versus controls by Student's *t*-test. **C**: Expression of androgen receptor (AR) and β-actin (loading control) in whole cell lysate proteins of LNCaP, LN95, LN-EV, and LN-HI cells was examined by Western blot analysis.

protein level of HMGA1 was reduced to 25% in DU145 cells and PC-3 cells compared with controls transfected with scrambled control siRNAs (Fig. 5A). Cell proliferation was measured by one WST-8 assay in androgen-deprived medium following the transfection of siRNAs. Knockdown of HMGA1 protein in DU145 cells by siRNA lead to the decrease in the cell proliferation rate by 40% 4 days after the transfection of siRNA compared with the controls transfected with scramble control siRNA (Fig. 5B). Similarly, a

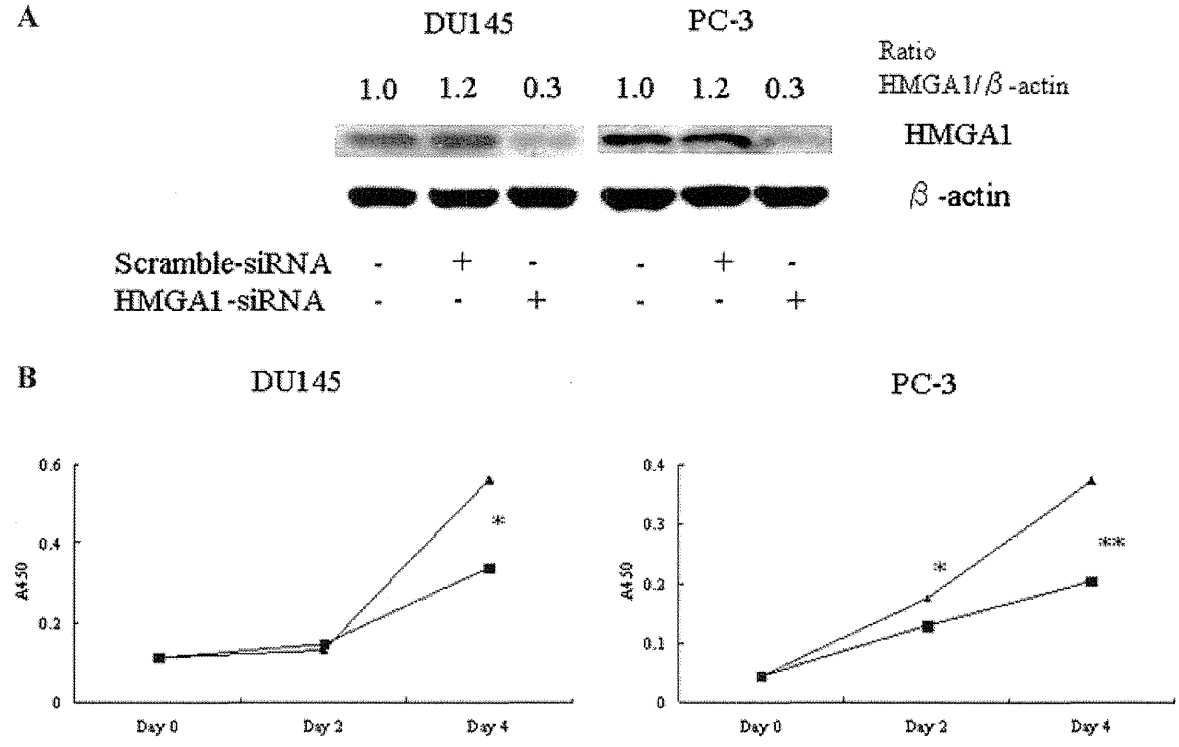

Fig. 5. Knockdown of HMGAI suppressed the cell growth of DUI45 and PC-3 in androgen-deprived condition. **A**: Knockdown of HMGAI in DUI45 and PC-3 cells. Whole cell lysate was prepared 2 days after transfection with the siRNAs. Expression of HMGAI and β-actin (loading control) in whole cell lysate proteins was examined by Western blot analysis. **B**: Cell growth curves for DUI45 and PC-3 cells transfected with scramble-siRNA (▲) and HMGAI-siRNA (■). Cells in androgen-deprived medium were transfected with siRNAs on day 0. Suppression of HMGAI by siRNA in DUI45 cells decreased the cell proliferation rate at day 4 by 40%. Similarly, a 45% decrease was observed for PC-3 cells. Values are means ± SD. $^{*}P < 0.05$; $^{**}P < 0.001$ versus controls by Student's *t*-test.

decrease of cell proliferation rate by 45% compared with controls transfected with scramble control siRNA was observed 4 days after the transfection of HMGA1 siRNA in PC-3 cells. Knockdown of HMGA1 by siRNA suppressed the cell proliferation of androgen-independent PCa cells, DU145 and PC-3, under androgen-deprived condition.

DISCUSSION

Metastasis, chromosomal instability, and androgen independent growth are hallmark features of advanced PCa. Previous reports suggest that HMGA1 is associated with high stage and invasive human PCa [8,9] and with the metastatic potential of Dunning rat PCa cells [15]. We previously reported that the overexpression of HMGA1 induces the expression of matrix metalloproteinase 2, which is related to cell invasion potential, in PCa cells [11]. We also reported that the expression of HMGA1 in the TRAMP is confined to the later stage when metastatic lesions are formed [12]. In addition, our previous report suggests that HMGA1 is a candidate protein for chromosomal rearrangements in human PCa cells [10]. These findings suggest that HMGA1 is a strong candidate gene playing a potential role in the progression of PCa.

In the present study, we examined how HMGA1 plays a role in the development of androgen-independence, which is an important biological features acquired during the progression to advanced PCa. The current study indicated that the high level of HMGA1 expression is associated with androgen-independent PCa cell lines including not only AR-negative DU145 and PC-3 cells but also AR-positive androgen-independent LN95 cells, established by maintaining LNCaP cells in the absence of androgens for long periods of time. Our in vitro and in vivo experiments demonstrated that androgen-deprivation induced the increased expression of HMGA1 exclusively in LNCaP cells but not in normal prostate tissue. This suggests that ADT might induce increased expression of HMGA1, a molecule potentially associated with the progression of PCa, in a certain population of androgen-sensitive PCa cells. Furthermore, the

current study demonstrated that overexpression of HMGA1 in LNCaP cells attenuated the suppression of cell proliferation under androgen-deprived condition. Both the LNCaP cells transfected with HMGA1a vector (LN-H1) and the LNCaP cells transfected with control empty vector (LN-EV) grew equally well in the presence of androgen. In contrast, LN-H1 cells but not LN-EV cells could maintain cell proliferation even under androgen-deprived or low androgen conditions. This suggests that up-regulated HMGA1 in androgen-dependent PCa cells might contribute to the cell proliferation and cell survival during ADT. In this study, RNA interference experiments demonstrated that knockdown of HMGA1 in DU145 and PC-3 cells significantly inhibited the cell proliferation. This finding suggests that HMGA1 plays an important role in the cell proliferation of androgen-independent PCa cells and that HMGA1 might be a possible target molecule for novel therapeutic modalities for CRPC.

Hypoxia [16], 12-*O*-tetradecanoylphorbol-13-aettarte (TPA) [17], interleukin-1β [18], and c-Myc [19] have been reported to induce the expression of HMGA1. This study is the first to suggest that androgen manipulation also affects the induction of HMGA1. Since androgen-deprivation induced the expression of HMGA1, it is speculated that the transcription of HMGA1 is directly regulated by AR in association with co-factors or by some other transcriptional factors whose expression is regulated by AR signaling pathway.

There are few reports suggesting a correlation between HMGA1 and sex hormones. Massaad-Massade et al. reported that HMGA1 enhanced the transcriptional activity and binding of estrogen receptor to its responsive element [20], suggesting a protein–protein interaction between HMGA1 and estrogen receptor. This leads us to speculate the possibility that HMGA1 in analogy enhances the transcriptional activity and binding of AR to the androgen responsive element (ARE). If this synergistic activation of the ARE is observed even in the absence of or under the very low concentration of androgen, the increased expression of HMGA1 should contribute to the acquisition of androgen-independence by AR-positive PCa cells. Further experiments are warranted to confirm this hypothesis. Dysregulation of AR is one of the major mechanisms involved in the development of androgen independent PCa cells [21]. Recently, AR spliced variants with truncation have gained a particular attention, since several reports have demonstrated that the expression of the AR spliced variants is induced by androgen-deprivation and it also plays an important role in CRPC [22,23]. Therefore, we also examined the expression status of AR in LN-H1 cells (LNCaP overexpressing HMGA1) in comparison with parental LNCaP cells, LN-EV cells (LNCaP transfected with control empty vector), and LN95 cells (androgen-independent LNCaP subline maintained in the absence of androgens) by Western blot. LN95 expressed not only full-length AR but also ~75-kDa AR, which appears to be the previously reported AR spliced variant. In contrast, both LN-EV and LN-H1 expressed only full-length AR but not AR spliced variant. The AR expression levels in LN-EV, LN-H1, and LN95 were very similar and about twofold the level in parental LNCaP. Androgen-deprivation induced the expression of both HMGA1 and AR spliced variant in LNCaP, while simple overexpression of HMGA1 did not induce the expression of AR spliced variant in LNCaP. Recent advances has identified several other possible mechanisms and pathways involved in the development of androgen-independent PCa (i.e., CRPC). Among these, the induction pattern and speculated role of NF-κB/p52 and syncecan-1 (CD138) are similar to those of HMGA1. NF-κB/p52 activation has been reported to induce androgen-independent growth of LNCaP by protecting the cells from apoptosis and cell cycle arrest induced by androgen-deprivation [24]. However, it is not clarified in the paper whether activation or increased expression of NF-κB/p52 is induced by androgen-deprivation. Shimada et al. has reported that androgen-deprivation induced expression of syndecan-1 (CD138)

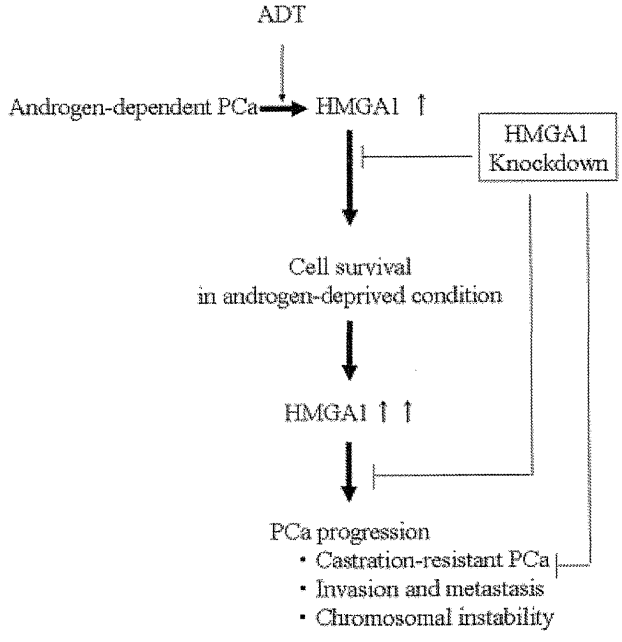

Fig. 6. Expression and roles of HMGA1 in the development of androgen-dependent into androgen-independent prostate cancer. ADT: androgen-deprivation therapy, PCa: prostate cancer.

in androgen sensitive LNCaP cells and plays a role in cell proliferation of androgen-independent DU145 and PC-3 [25]. Even though the molecular functions are different, these molecules may contribute in concert to the development of CRPC.

Based on the findings demonstrated in this study, we speculate the roles of HMGA1 in the development of androgen-independent PCa in clinical settings as illustrated in Figure 6. While the majority of androgen dependent PCa is eliminated by ADT, the expression of HMGA1 is induced in a minority of clones. The increased HMGA1 in such clones promotes cell proliferation under androgen deprived conditions during ADT, which results in the development of androgen-independent clones. In addition, after acquiring androgen-independency HMGA1 plays a role in the cell proliferation of CRPC. Based on these speculations, HMGA1 is suggested to be a potential target molecule for preventing the transition from androgen-dependent to androgen-independent cancer as well as for therapy of CRPC. Further elucidation of the molecular mechanism regarding the above mentioned findings are warranted to confirm the role of HMGA1 in the development of androgen-independent PCa.

CONCLUSIONS

In conclusion, it is suggested that HMGA1 is induced by androgen-deprivation, is involved in the development of androgen-dependent into androgen-independent PCa, and also plays a significant role in the cell proliferation of androgen-independent PCa cells. These findings make HMGA1 a potential candidate target molecule of prevention and therapy for CRPC.

ACKNOWLEDGMENTS

We thank Y. Morioka, C. Tsukisato, and K. Koishihara for their technical assistance. We thank Dr. Allan Meeker for providing us LN95 cell line. We acknowledge Dr. Robert Getzenberg for providing LN-EV and LN-H1 cell lines.

REFERENCES

1. Jemal A, Siegel R, Ward E, Hao Y, Xu J, Thun MJ. Cancer statistics, 2009. CA Cancer J Clin 2009;59(4):225–249.
2. Fusco A, Fedele M. Roles of HMGA proteins in cancer. Nat Rev Cancer 2007;7(12):899–910.
3. Reeves R, Nissen MS. The A.T-DNA-binding domain of mammalian high mobility group I chromosomal proteins. A novel peptide motif for recognizing DNA structure. J Biol Chem 1990;265(15):8573–8582.
4. Frasca F, Rustighi A, Malaguarnera R, Altamura S, Vigneri P, Del Sal G, Giancotti V, Pezzino V, Vigneri R, Manfioletti G. HMGA1 inhibits the function of p53 family members in thyroid cancer cells. Cancer Res 2006;66(6):2980–2989.
5. Ueda Y, Watanabe S, Tei S, Saitoh N, Kuratsu J, Nakao M. High mobility group protein HMGA1 inhibits retinoblastoma protein-mediated cellular G0 arrest. Cancer Sci 2007;98(12): 1893–1901.
6. Chiappetta G, Avantaggiato V, Visconti R, Fedele M, Battista S, Trapasso F, Merciai BM, Fidanza V, Giancotti V, Santoro M, Simeone A, Fusco A. High level expression of the HMGI (Y) gene during embryonic development. Oncogene 1996;13(11): 2439–2446.
7. Evans A, Lennard TW, Davies BR. High-mobility group protein 1(Y): Metastasis-associated or metastasis-inducing? J Surg Oncol 2004;88(2):86–99.
8. Tamimi Y, van der Poel HG, Denyn MM, Umbas R, Karthaus HF, Debruyne FM, Schalken JA. Increased expression of high mobility group protein I(Y) in high grade prostatic cancer determined by in situ hybridization. Cancer Res 1993;53(22): 5512–5516.
9. Tamimi Y, van der Poel HG, Karthaus HF, Debruyne FM, Schalken JA. A retrospective study of high mobility group protein I(Y) as progression marker for prostate cancer determined by in situ hybridization. Br J Cancer 1996;74(4):573–578.
10. Takaha N, Hawkins AL, Griffin CA, Isaacs WB, Coffey DS. High mobility group protein I(Y): A candidate architectural protein for chromosomal rearrangements in prostate cancer cells. Cancer Res 2002;62(3):647–651.
11. Takaha N, Resar LM, Vindivich D, Coffey DS. High mobility group protein HMGI(Y) enhances tumor cell growth, invasion, and matrix metalloproteinase-2 expression in prostate cancer cells. Prostate 2004;60(2):160–167.
12. Leman ES, Madigan MC, Brunagel G, Takaha N, Coffey DS, Getzenberg RH. Nuclear matrix localization of high mobility group protein I(Y) in a transgenic mouse model for prostate cancer. J Cell Biochem 2003;88(3):599–608.
13. Pflug BR, Reiter RE, Nelson JB. Caveolin expression is decreased following androgen deprivation in human prostate cancer cell lines. Prostate 1999;40(4):269–273.
14. Kolb S, Fritsch R, Saur D, Reichert M, Schmid RM, Schneider G. HMGA1 controls transcription of insulin receptor to regulate cyclin D1 translation in pancreatic cancer cells. Cancer Res 2007;67(10):4679–4686.
15. Bussemakers MJ, van de Ven WJ, Debruyne FM, Schalken JA. Identification of high mobility group protein I(Y) as potential progression marker for prostate cancer by differential hybridization analysis. Cancer Res 1991;51(2):606–611.
16. Ji YS, Xu Q, Schmedtje JF Jr. Hypoxia induces high-mobility-group protein I(Y) and transcription of the cyclooxygenase-2 gene in human vascular endothelium. Circ Res 1998;83(3):295–304.
17. Cmarik JL, Li Y, Ogram SA, Min H, Reeves R, Colburn NH. Tumor promoter induces high mobility group HMG-Y protein expression in transformation-sensitive but not-resistant cells. Oncogene 1998;16(26):3387–3396.
18. Pellacani A, Chin MT, Wiesel P, Ibanez M, Patel A, Yet SF, Hsieh CM, Paulauskis JD, Reeves R, Lee ME, Perrella MA. Induction of high mobility group-I(Y) protein by endotoxin and interleukin-1beta in vascular smooth muscle cells. Role in activation of inducible nitric oxide synthase. J Biol Chem 1999;274(3):1525–1532.
19. Wood LJ, Mukherjee M, Dolde CE, Xu Y, Maher JF, Bunton TE, Williams JB, Resar LM. HMG-I/Y, a new c-Myc target gene and potential oncogene. Mol Cell Biol 2000;20(15):5490–5502.

20. Massaad-Massade L, Navarro S, Krummrei U, Reeves R, Beaune P, Barouki R. HMGA1 enhances the transcriptional activity and binding of the estrogen receptor to its responsive element. Biochemistry 2002;41(8):2760–2768.
21. Debes JD, Tindall DJ. Mechanisms of androgen-refractory prostate cancer. N Engl J Med 2004;351(15):1488–1490.
22. Sun S, Sprenger CC, Vessella RL, Haugk K, Soriano K, Mostaghel EA, Page ST, Coleman IM, Nguyen HM, Sun H, Nelson PS, Plymate SR. Castration resistance in human prostate cancer is conferred by a frequently occurring androgen receptor splice variant. J Clin Invest 2010;120(8):2715–2730.
23. Watson PA, Chen YF, Balbas MD, Wongvipat J, Socci ND, Viale A, Kim K, Sawyers CL. Constitutively active androgen receptor splice variants expressed in castration-resistant prostate cancer require full-length androgen receptor. Proc Natl Acad Sci USA 2010;107(39):16759–16765.
24. Nadiminty N, Chun JY, Lou W, Lin X, Gao AC. NF-kappaB2/p52 enhances androgen-independent growth of human LNCaP cells via protection from apoptotic cell death and cell cycle arrest induced by androgen-deprivation. Prostate 2008;68(16):1725–1733.
25. Shimada K, Nakamura M, De Velasco MA, Tanaka M, Ouji Y, Konishi N. Syndecan-1, a new target molecule involved in progression of androgen-independent prostate cancer. Cancer Sci 2009;100(7):1248–1254.

nature medicine

Multipeptide immune response to cancer vaccine IMA901 after single-dose cyclophosphamide associates with longer patient survival

Steffen Walter[1,21], Toni Weinschenk[1,21], Arnulf Stenzl[2], Romuald Zdrojowy[3], Anna Pluzanska[4], Cezary Szczylik[5], Michael Staehler[6], Wolfram Brugger[7], Pierre-Yves Dietrich[8], Regina Mendrzyk[1], Norbert Hilf[1], Oliver Schoor[1], Jens Fritsche[1], Andrea Mahr[1], Dominik Maurer[1], Verona Vass[1], Claudia Trautwein[1], Peter Lewandrowski[1], Christian Flohr[1], Heike Pohla[9,10], Janusz J Stanczak[11], Vincenzo Bronte[12], Susanna Mandruzzato[13,14], Tilo Biedermann[15], Graham Pawelec[16], Evelyna Derhovanessian[16], Hisakazu Yamagishi[17], Tsuneharu Miki[18], Fumiya Hongo[18], Natsuki Takaha[18], Kosei Hirakawa[19], Hiroaki Tanaka[19], Stefan Stevanovic[20], Jürgen Frisch[1], Andrea Mayer-Mokler[1], Alexandra Kirner[1], Hans-Georg Rammensee[20], Carsten Reinhardt[1,21] & Harpreet Singh-Jasuja[1,21]

IMA901 is the first therapeutic vaccine for renal cell cancer (RCC) consisting of multiple tumor-associated peptides (TUMAPs) confirmed to be naturally presented in human cancer tissue. We treated a total of 96 human leukocyte antigen A (HLA-A)*02$^+$ subjects with advanced RCC with IMA901 in two consecutive studies. In the phase 1 study, the T cell responses of the patients to multiple TUMAPs were associated with better disease control and lower numbers of prevaccine forkhead box P3 (FOXP3)$^+$ regulatory T (T_{reg}) cells. The randomized phase 2 trial showed that a single dose of cyclophosphamide reduced the number of T_{reg} cells and confirmed that immune responses to multiple TUMAPs were associated with longer overall survival. Furthermore, among six predefined populations of myeloid-derived suppressor cells, two were prognostic for overall survival, and among over 300 serum biomarkers, we identified apolipoprotein A-I (APOA1) and chemokine (C-C motif) ligand 17 (CCL17) as being predictive for both immune response to IMA901 and overall survival. A randomized phase 3 study to determine the clinical benefit of treatment with IMA901 is ongoing.

Therapeutic cancer vaccines hold the promise of combining meaningful efficacy (prolongation of survival) with very good safety and tolerability, as has been shown in several recent randomized trials[1–3]. However, development of cancer vaccines remains a major challenge, with little knowledge of (i) the optimal tumor antigens to target, (ii) suitable agents to counteract regulatory mechanisms opposing successful immunotherapy and (iii) surrogate and predictive biomarkers that can improve our understanding of these regulatory mechanisms and predict a patient's response to therapy.

The first major issue addressed in this work is whether relevant HLA-restricted peptides for immunotherapeutic intervention in patients with RCC can be identified and clinically validated. We defined the relevance of the antigens as their natural presence on the tumor in the majority of RCC samples, their immunogenicity (induction of T cell responses in clinical studies) and the association of the vaccine-induced T cell responses with clinical benefit. For the identification, selection and preclinical immunological validation of such antigens, we used the antigen discovery platform XPRESIDENT[4,5] to create a multipeptide vaccine designated IMA901 for immunotherapy of RCC. We tested IMA901 in HLA-A*02$^+$ subjects with advanced RCC in two clinical trials, a phase 1 ($n = 28$) and a randomized phase 2 ($n = 68$) trial, both of which assessed the association of T cell responses to IMA901 with clinical benefit.

[1]Immatics Biotechnologies GmbH, Tübingen, Germany. [2]Department of Urology, Eberhard Karls University Tübingen, Tübingen, Germany. [3]Department of Urology and Urological Oncology, University of Medicine, Wroclaw, Poland. [4]Klinika Chemiotherapii Nowotworow UM, Uniwersytetu Medycznego, Lodz, Poland. [5]Department of Oncology, Military Institute of Medicine, Warsaw, Poland. [6]Interdisziplinäres Zentrum für Nierentumore (IZN), Ludwig Maximilians University, Munich, Germany. [7]Department of Hematology, Oncology & Immunology, Schwarzwald-Baar Klinikum and Academic Teaching Hospital of the University of Freiburg, Villingen-Schwenningen, Germany. [8]Laboratory of Tumour Immunology, Centre of Oncology, University Hospital of Geneva, Geneva, Switzerland. [9]Laboratory of Tumor Immunology, LIFE Center, Ludwig Maximilians University, Munich, Germany. [10]Institute of Molecular Immunology, Helmholtz Center, Munich, Germany. [11]Molecular Diagnostics Laboratory, Hospital for Infectious Diseases, Warsaw, Poland. [12]Department of Pathology and Diagnostics, Verona University Hospital, Verona, Italy. [13]Department of Surgery, Oncology and Gastroenterology, University of Padova, Padova, Italy. [14]Istituto Oncologico Veneto (IOV) Istituto Di Ricovero e Cura a Carattere Scientifico (IRCCS), Padova, Italy. [15]Department of Dermatology, Eberhard Karls University Tübingen, Tübingen, Germany. [16]Department of Internal Medicine II, Centre for Medical Research, Eberhard Karls University Tübingen, Tübingen, Germany. [17]Department of Surgery, Kyoto Prefectural University of Medicine, Kyoto, Japan. [18]Department of Urology, Kyoto Prefectural University of Medicine, Kyoto, Japan. [19]Department of Surgical Oncology, Osaka City University, Osaka, Japan. [20]Department of Immunology, Eberhard Karls University Tübingen, Tübingen, Germany. [21]These authors contributed equally to this work. Correspondence should be addressed to H.S.-J. (singh@immatics.com).

Received 28 February; accepted 20 June; published online 29 July 2012; doi:10.1038/nm.2883

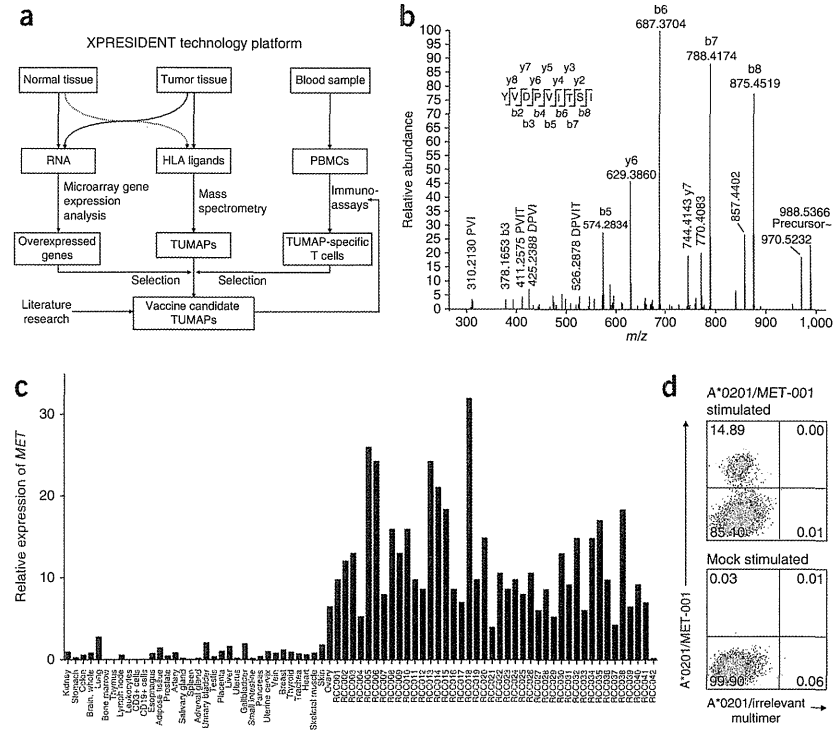

Figure 1 Key components of the XPRESIDENT technology platform to identify and select naturally presented TUMAPs. (**a**) Process scheme showing the steps from primary tumor tissues and blood samples to a multipeptide immunotherapeutic cancer vaccine. (**b**) Shown as an example is the sequencing of the peptide YVDPVITSI (MET-001) encoded by *MET* and naturally presented by HLA-A*02 on primary RCC tissue by mass spectrometry. *m/z*, mass to charge ratio; b2–b8, b-series fragment ions; y2–y8, y-series fragment ions. (**c**) mRNA expression profile of *MET*. Expression values for bulk normal tissues and several RCC samples are shown relative to normal bulk kidney (with a value arbitrarily set to 1.0). Each bar represents a single microarray measurement. (**d**) HLA multimer analysis of *in vitro*–primed T cells generated by stimulation of human CD8$^+$ T cells derived from healthy donors with MET-001 (top) or an irrelevant peptide (bottom) using artificial antigen-presenting cells. The numbers in the quadrants indicate the percentage of CD8$^+$ cells.

The second aim was to identify an agent that reduced numbers of T_{reg} cells and that improved the clinical efficacy of the vaccine. A single dose of cyclophosphamide has been used in several previous studies with the intention of inhibiting T_{reg} cells[6–9]. However, a beneficial effect of single-dose cyclophosphamide had not previously been conclusively shown in a randomized clinical trial.

The third issue addressed was whether blood cell populations or serum factors could be identified as prognostic or predictive biomarkers. We investigated cell populations known to counteract T cell–based immunotherapy, such as T_{reg} cells[10], several populations of myeloid-derived suppressor cells (MDSCs)[11,12], interleukin-10 (IL-10)-secreting and IL-17–secreting T cells[13] and dysfunctional T cell receptor ζ (TCR-ζ)^{low} or nitrotyrosine^{high} T cells[14,15], which might have an effect on the prognosis of patients with RCC. Lastly, we also screened >300 serum biomarkers for association with clinical outcome and immune response.

RESULTS

Identification of TUMAPs based on natural presentation

XPRESIDENT is an antigen discovery platform that allows for the identification of thousands of TUMAPs—collectively defined as the HLA ligandome or immunopeptidome—directly from primary tumor tissues (**Fig. 1a**). It uses a combination of mass spectrometry, gene expression profiling, literature-based functional assessment, *in vitro* human T cell assays and bioinformatics to select a set of candidate vaccine TUMAPs for the tumor type of interest[4,16,17].

We systematically investigated 80 predominantly primary RCC tissues, including 32 evaluable HLA-A*02$^+$ RCC samples, by mass spectrometry, resulting in the identification of peptides from housekeeping and tumor-associated antigens[4,18]. To identify potentially clinically relevant antigens, we compared the mRNA expression profiles of 42 RCC samples to those of 35 different healthy tissues[19] and tested the immunogenicity of candidate tumor-associated antigens determined by gene expression profiling through subsequent *in vitro* priming using artificial antigen-presenting cells[16] to detect antigen-specific T cells in peripheral blood cells of healthy donors. We selected nine HLA-A*02–restricted TUMAPs and one HLA-DR–restricted TUMAP that were derived from highly overexpressed tumor antigens and designated them IMA901 (**Table 1**). We added an HLA-A*02–restricted peptide from hepatitis B virus (HBV) as a marker peptide for the phase 1 study[20] that was not part of the IMA901 formulation in further trials. Data from a representative TUMAP, MET-001, are shown in **Figure 1b–d**.

Safety, immunogenicity and efficacy in the phase 1 study

To investigate safety and obtain preliminary results on the immunogenicity and potential clinical benefit of IMA901 in humans, we conducted an open-label, multicenter, single-arm phase 1 study in patients with advanced RCC. Subjects received up to eight IMA901 vaccinations, each preceded by administration of granulocyte-macrophage colony-stimulating factor (GM-CSF) as an immunomodulator (**Fig. 2a**). We enrolled 28 HLA-A*02$^+$ subjects with RCC, 15 of whom had not received prior systemic treatment. The remaining 13 subjects had previously received up to three treatment lines, mostly consisting of cytokines, often in combination with chemotherapy. We observed no treatment-related serious adverse events or deaths during the study period. At a 3-month follow up, disease had progressed in 16 subjects, 11 subjects had stable disease and 1 subject showed a partial response to therapy according to the Response Evaluation Criteria in Solid Tumors (RECIST).

Among 27 immune-evaluable subjects, 20 showed a vaccine-induced T cell response to at least one TUMAP and 8 responded to multiple TUMAPs. Fourteen subjects showed a response to the HBV-001 marker peptide. As detailed in the Online Methods, we analyzed responses after a single round of *in vitro* stimulation and culture to enable the detection of both low and high frequencies of vaccine-induced T cells in the peripheral blood of the subjects. The kinetics of the T cell responses determined at the time points of individual blood drawings before and throughout the course of the

Table 1 Composition of the vaccine IMA901 and characteristics of the HBV peptide included in the phase 1 study

Peptide	Antigen	HLA	Overexpression	*In vitro* immunogenicity	Remarks on function and tumor relevance	References
ADF-001 (SVASTITGV)	PLIN2	A*02	6.0	+	Major constituent of the surface of lipid droplets.	4,49
ADF-002 (VMAGDIYSV)	APOL1	A*02	6.0	+	Overexpressed in several cancers; established as a marker for RCC.	
APO-001 (ALADGVQKV)		A*02	7.0	+	Secreted major apoprotein of high-density lipoprotein. Overexpression in RCC.	4
CCN-001 (LLGATCMFV)	CCND1	A*02	3.0	+	Cell cycle regulation. Overexpression and association with tumorigenesis and metastasis described for various tumors.	4,50
GUC-001 (SVFAGVVGV)	GUCY1A3	A*02	2.2	+	cGMP synthesis. Proangiogenic effects in tumors.	4
K67-001 (ALFDGDPHL)	PRUNE2	A*02	3.4	+	Largely uncharacterized so far. Overexpression in RCC.	4,18
MET-001 (YVDPVITSI)	MET	A*02	13.6	+	Hepatocyte growth factor receptor tyrosine kinase, cell signaling. Various implications in malignant transformation and invasiveness of tumor cells.	4,18,51
MUC-001 (STAPPVHNV)	MUC1	A*02	1.6	+	Protection against pathogen binding to the cell surface; roles in cell signaling. Altered glycosylation patterns lead to new T cell epitopes in tumors.	52–55
RGS-001 (LAALPHSCL)	RGS5	A*02	3.5	+	Regulation of cell signaling. Overexpression during neovascularization in tumors.	18,56
MMP-001 (SQDDIKGIQKLYGKRS)	MMP7	DR	3.3	+	Breakdown of extracellular matrix during tissue remodeling. Involved in tumor invasion and metastasis, tumor development and progression. Also, roles in apoptosis, cell proliferation and cell differentiation.	57
HBV-001 (FLPSDFFPSV)	HBV; nucleocapsid protein (HBcAg)	A*02	NA	+	Marker peptide, not tumor associated. HBcAg is an antigenic determinant of HBV. Serological responses develop in most HBV-infected subjects, used for diagnosis of infection.	20,58

The characteristics of individual peptides contained in IMA901 are shown with peptide code (sequence), source antigen, HLA restriction, overexpression, *in vitro* immunogenicity, remarks on function and references. In the "overexpression" column, the ratios of mean expression in all analyzed RCC samples ($n = 20$) compared with the mean expression in normal tissues are shown. In the column "*in vitro* immunogenicity," "+" indicates that *in vitro* expansion of peptide-specific T cells was observed. NA, not applicable.

vaccinations were analyzed for 13 response courses in 9 subjects in detail and are shown for a representative subject in **Figure 2b**. We typically observed peak responses at 1–3 weeks after start of vaccinations, and we were still able to detect vaccine-induced immune responses 3 months after start of vaccinations in 7 of 13 response courses.

In a retrospective analysis, we found that subjects who responded to multiple TUMAPs were significantly ($P = 0.019$) more likely to experience disease control (stable disease or partial response) than subjects who responded to only one TUMAP or had no response (**Fig. 2c**). In contrast, we found no association between T cell responses to HBV-001 and clinical benefit. To assess whether T_{reg} cells have a role in compromising immune responses in patients, we quantified the number of T_{reg} cells in the subjects before and after vaccination. Low percentages of T_{reg} cells before vaccination were associated with multiple T cell responses to the vaccine in comparison with nonresponders or single TUMAP immune responders (**Fig. 2d**; $P = 0.016$).

Safety and efficacy in the phase 2 study

We based the design of the phase 2 study on the observed positive association between disease control and T cell responses to multiple TUMAPs, as well as the negative association of T_{reg} cell numbers with the induction of such responses. We investigated whether an additional immunomodulator (single-dose cyclophosphamide) could improve the efficacy of IMA901 vaccination and the clinical outcome in patients with RCC, presumably by reducing the numbers of T_{reg} cells (**Fig. 3a**).

We randomized 1:1 a total of 68 HLA-A*02$^+$ subjects with metastatic RCC (intention-to-treat population, ITT) with documented progression during or after previous systemic therapy to receive either single-dose cyclophosphamide before the first of 17 vaccinations or no pretreatment (33 subjects comprised the arm that included pretreatment with cyclophosphamide, termed here the '+Cy arm', and 35 subjects comprised the arm with no pretreatment, termed here the '–Cy arm'); 64 subjects were evaluable for the predefined primary efficacy analysis (per protocol). The baseline characteristics and risk factors of the subjects were well balanced overall between the two randomization arms (**Supplementary Table 1**), except for a shorter median time since diagnosis in the subjects from the +Cy arm (which was reported to be a negative prognostic factor in previous studies[21,22]).

Confirming the phase 1 results, treatment with IMA901 was safe and generally well tolerated, with mild to moderate local site reactions being the most frequent side effects. Two possibly related serious adverse events were reported, with one subject experiencing a systemic allergic reaction after the twelfth vaccination (caused by GM-CSF, as shown by an *in vitro* basophil degranulation assay) and another with a grade 3 localized allergic reaction after the eleventh vaccination, with no similar signs of intolerance after further vaccinations. We found no differences in the safety profile between subjects in the +Cy arm and those in the –Cy arm.

Similar to reports for other cancer vaccines, shrinkage of established tumor lesions was infrequent, with one complete response and two partial responses being reported by investigators and one partial response as assessed by centralized review. The disease control rate (DCR; percentage of subjects with complete or partial response or stable disease according to RECIST within all treated subjects), according to a centralized review at 6 months after the start of treatment, was 31% (95% confidence interval (CI) 17–48%) in subjects with prior cytokine treatment and was 14% (95% CI 3–35%) in subjects

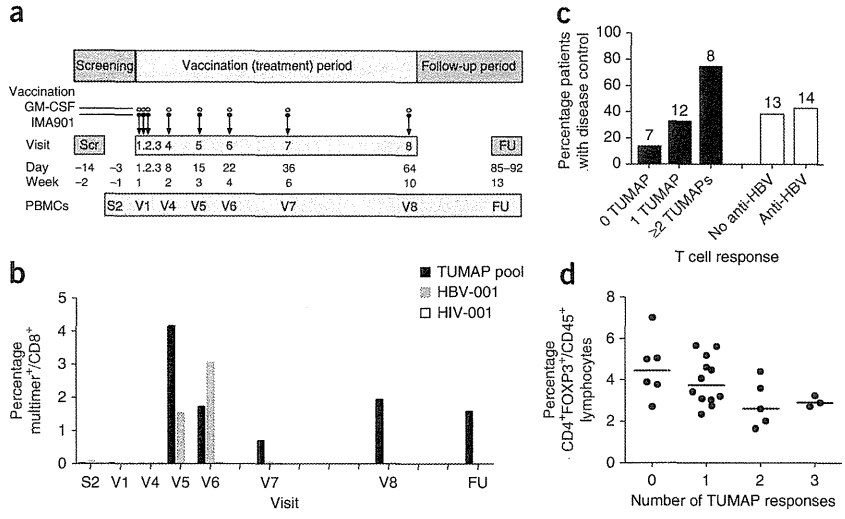

Figure 2 Key observations of the IMA901 phase 1 trial. (**a**) Schedule of vaccinations with IMA901 plus the immunomodulator GM-CSF and of peripheral blood mononuclear cell (PBMC) sampling. Scr, screening; V, vaccination; FU, follow up (no vaccine applied). (**b**) The observed magnitude of T cell kinetics in a multimer analysis of a representative subject vaccinated with IMA901. The readout antigens were nine HLA class I TUMAPs in one sample (TUMAP pool), the marker peptide HBV-001, which was included in IMA901, and the negative control antigen HIV-001, which was not included in the vaccine. The timeline is shown in weeks, with each tick indicating 1 week. (**c**) DCR of subjects according to the presence or absence of detectable immune responses ($n = 27$ subjects total). The numbers above the bars indicate number of subjects with the observed immune responses. Anti-HBV, vaccine-induced response to the HBV peptide. (**d**) Association of the number of T cell responses with the percentage of T_{reg} cells ($n = 26$ subjects). Shown on the *y* axis is the percentage of $CD4^+FOXP3^+$ cells among $CD45^+$ lymphocytes in prevaccination samples. Shown on the *x* axis is the number of vaccine-induced TUMAP responses per subject. Each dot represents an individual subject, and the horizontal lines represent the median values.

with prior tyrosine kinase inhibitor (TKI) treatment. Whereas progression-free survival (PFS) was comparable in the two study arms (**Fig. 3b**), we found a trend for prolonged survival in subjects in the +Cy arm (median overall survival of 23.5 months for +Cy compared with 14.8 months for −Cy, hazard ratio (HR) = 0.57, $P = 0.090$; **Fig. 3c** and **Supplementary Table 1**).

Association of immune responses and overall survival

Of the 64 per protocol subjects, 61 were evaluable for a prospectively defined immune response analysis. The immune response rate of 64% in this group (including 26% multi-TUMAP responders) was similar to that of the phase 1 study (where we investigated more time points).

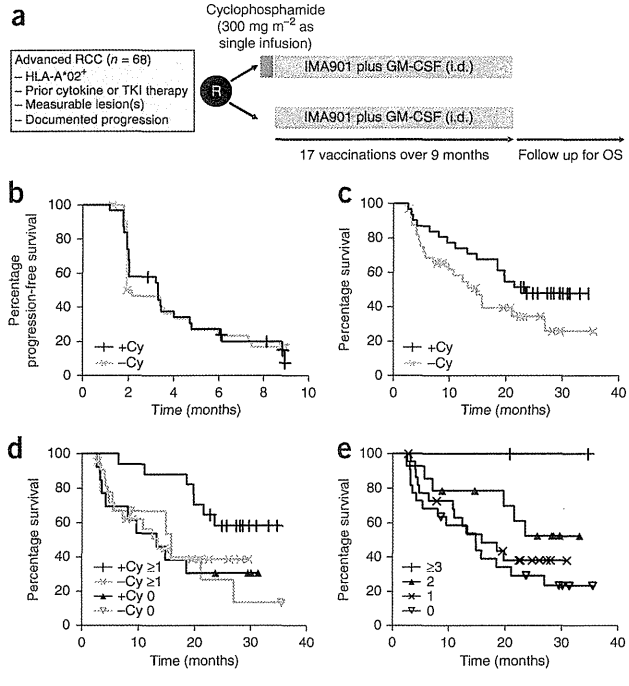

These rates were comparable between subjects with and without cyclophosphamide pretreatment (data not shown), indicating that cyclophosphamide did not alter the induction of T cell responses.

The baseline characteristics of the subjects were generally well balanced between the immune responders and the nonresponders and between multi-TUMAP responders and single-TUMAP responders or nonresponders (**Supplementary Table 2**). However, age was associated with fewer multi-TUMAP responses ($P = 0.01$), and there was a tendency toward more responses in male than in female subjects. Neither age nor gender have otherwise been reported as prognostic factors for overall survival of patients with RCC[22].

Despite the observed similarity of prognostic factors in the subjects in the +Cy and −Cy arms, a prospectively defined analysis showed that among immune responders, subjects had prolonged survival if pretreated with cyclophosphamide compared with subjects without this pretreatment (HR = 0.38, $P = 0.040$) (**Fig. 3d**). In contrast, we found no difference in survival of subjects in the +Cy and −Cy arms among nonimmune responders (HR = 0.92, $P = 0.870$). Although these data are based on small numbers of subjects because of the trial design, they suggest that a single dose of cyclophosphamide does not have antitumor activity by itself but instead supports the effects of the vaccine as an immunomodulator and enables the translation of immune responses into clinical benefit. Furthermore, survival time was extended if a subject had a response to multiple TUMAPs ($P = 0.023$

Figure 3 Overall survival and PFS of subjects treated in the phase 2 trial. Evaluable subjects of the per protocol population are shown in the survival curves. (**a**) Design of the clinical trial. OS, overall survival; R, randomization; i.d., intradermal administration. (**b**) PFS of subjects treated with ($n = 31$) or without ($n = 33$) cyclophosphamide. (**c**) Overall survival of subjects treated with ($n = 31$) or without ($n = 33$) cyclophosphamide. (**d**) Overall survival of subjects evaluable for immune responses grouped as follows: immune responders, +Cy arm ($n = 17$); subjects without an observed immune response, +Cy arm ($n = 13$); immune responders, −Cy arm ($n = 22$); subjects without an observed immune response, −Cy arm ($n = 9$). (**e**) Overall survival of subjects with no detectable immune responses ($n = 22$), immune responses to one TUMAP ($n = 23$), immune responses to two TUMAPs ($n = 14$) or immune responses to at least three TUMAPs ($n = 2$).

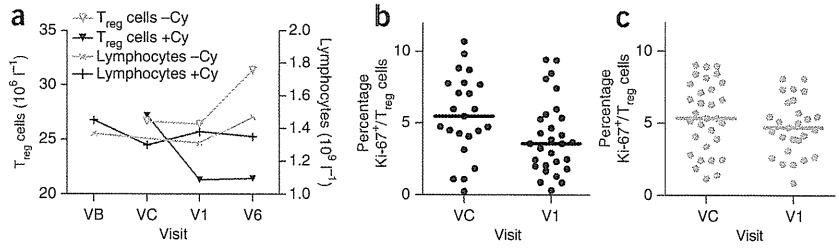

Figure 4 Modulation of T_{reg} cells by single-dose cyclophosphamide. (**a**) The medians of the absolute T_{reg} cell and lymphocyte counts of evaluable phase 2 subjects at different visits: VB, screening up to 4 weeks before V1; VC, administration of single-dose cyclophosphamide 3 d before V1; V1, first IMA901 vaccination; V6, sixth vaccination 3 weeks after V1. T_{reg} cells of evaluable ITT subjects pretreated with cyclophosphamide ($n = 25$ at VC, $n = 29$ at V1, $n = 28$ at V6), T_{reg} cells of subjects not pretreated with cyclophosphamide ($n = 31$ at VC, $n = 27$ at V1, $n = 27$ at V6), lymphocytes of subjects pretreated with cyclophosphamide ($n = 33$ at VB, $n = 31$ at VC, $n = 33$ at V1, $n = 32$ at V6) and lymphocytes of subjects not pretreated with cyclophosphamide ($n = 35$ at VB, $n = 35$ at V1, $n = 34$ at V6) are shown. The decrease in the numbers of T_{reg} cells from VC to V1 was significant in the +Cy arm ($P = 0.013$ by paired two-sided Wilcoxon test, $n = 24$). (**b**,**c**) Phenotype of circulating T_{reg} cells in evaluable subjects treated with cyclophosphamide (**b**) ($n = 23$ at VC, $n = 29$ at V1) or not treated with cyclophosphamide (**c**) ($n = 31$ at VC, $n = 27$ at V1). Frequency of Ki-67$^+$ cells among the T_{reg} cells was significantly decreased from VC to V1 in subjects treated with cyclophosphamide ($P = 0.0006$ by paired two-sided Wilcoxon test, $n = 23$). Each dot represents an individual subject, and the horizontal lines represent the median values.

log-rank test for trend in subjects with increasing number of responses) (**Fig. 3e**), corroborating the observation from the phase 1 study that clinical benefit is associated with the breadth of vaccine-induced immune responses.

Downmodulation of T_{reg} cells by cyclophosphamide

To assess the effects of single-dose cyclophosphamide on the numbers of T_{reg} cells in patients with RCC, we characterized these cells[23,24] as CD45$^+$CD3$^+$CD4$^+$CD8$^-$FOXP3$^+$CD25^{hi}CD127^{low} by immunophenotyping. A prospectively defined analysis showed an approximately 20% reduction in T_{reg} cell numbers 3 d after compared with immediately before the cyclophosphamide infusion in the +Cy arm ($P = 0.013$); we found no such effect in the –Cy arm and no effect on absolute lymphocyte counts in subjects from either arm (**Fig. 4a**).

Furthermore, quantifying the expression of Ki-67 showed that the percentage of proliferating cells among all T_{reg} cells was decreased 3 d after compared with before cyclophosphamide treatment (**Fig. 4b**,**c**).

Assessment of cellular biomarkers before treatment

To establish a profile of the immune-regulatory environment of patients with RCC, we analyzed different cellular biomarkers in samples from subjects of the phase 2 study obtained before treatment with cyclophosphamide and IMA901 and from matched healthy controls. MDSCs are myeloid cells with immunosuppressive properties that have been proposed to negatively modulate anticancer immunity. We developed a panel of antibodies to identify six MDSC phenotypes in a single multicolor staining: MDSC1 (CD14$^+$, interleukin-4 receptor α (IL-4Rα)$^+$)[25], MDSC2 (CD15$^+$IL-4Rα$^+$)[25], MDSC3 (Lineage$^-$HLA-DR$^-$CD33$^+$)[26,27], MDSC4 (CD14$^+$HLA-DR$^{-/lo}$)[28], MDSC5 (CD11b$^+$CD14$^-$CD15$^+$)[14] and MDSC6 (CD15$^+$FSC^{lo}SSC^{hi})[29]. We found that the percentage of MDSC2–MDSC6 phenotypes among all lymphocytes were significantly ($P < 0.01$) higher in subjects with RCC than in the controls (**Fig. 5a** and **Supplementary Fig. 1a–e**).

Two key mechanisms by which MDSCs cause T cell dysfunction have previously been reported: depletion of arginine, which induces T cell receptor ζ chain downregulation[14], and the generation of reactive oxygen species, which induces T cell tyrosine nitration[30,31]. Indeed, we found that TCR-ζ expression and nitrotyrosine expression by T cells—both measured as median fluorescence—were significantly lower ($P < 0.0001$) and higher ($P = 0.0038$), respectively, in patients compared with controls (**Fig. 5b**,**c**). TCR-ζ expression was significantly inversely correlated with numbers of MDSC2–MDSC4 ($P < 0.05$, data not shown) and strongly inversely correlated with MDSC5 ($P < 0.0001$; data not shown). We found no association between nitrotyrosine expression and the numbers of phenotypes MDSC1–MDSC6 (data not shown).

IL-17$^+$CD4$^+$ T cells (T helper type 17 (T_H17) cells) represent a distinct lineage of helper T cells with proinflammatory effector functions. T_H17 cells have been found to be elevated in several human cancers[13,32,33] and may predict metastatic progression[13]. Comparison of patients with RCC and controls (**Fig. 5d**,**e** and **Supplementary Fig. 1f**,**g**) showed that T_H17 cells were significantly enriched in the peripheral blood of subjects with RCC ($P < 0.0001$; **Fig. 5d**). Furthermore, the concentrations of IL-10$^+$CD4$^+$ T cells were also significantly higher in patients with RCC than in controls ($P < 0.0001$, **Fig. 5e**).

In a retrospective analysis, the numbers of two out of the six MDSC phenotypes were significantly negatively associated with overall survival: MDSC4 ($P < 0.001$ by continuous analysis; patients with high compared with low numbers of MDSC4 are shown in **Fig. 5f**) and MDSC5 ($P = 0.016$). TCR-ζ expression tended to associate positively with survival ($P = 0.084$).

Assessment of serum biomarkers before treatment

To identify serum parameters that could predict a potentially increased immunogenicity and overall survival by IMA901 treatment, we measured >300 analytes in samples from subjects in the IMA901 phase 2 study before treatment. To distinguish prognostic biomarkers (that is, those associated with clinical outcome independent of therapy) from predictive biomarkers, we considered only those biomarkers that were associated with both immune response and with overall survival in the +Cy arm but not in the –Cy arm. The use of this method was justified by the observation that immune responses to TUMAPs were associated with clinical benefit in both clinical studies described here (whereas responses to HBV-001 were not) and by the finding that subjects from the +Cy arm showed longer overall survival times (HR = 0.57, $P = 0.090$) and better association of immune response with overall survival compared with subjects in the –Cy arm.

Post-hoc univariate statistical analyses revealed that serum concentrations of two analytes, APOA1 and CCL17, were positively predictive for immune responses ($P = 0.016$ and $P = 0.032$, respectively) and multipeptide responses ($P < 0.0001$ and $P = 0.0028$, respectively; data not shown). High concentrations of APOA1 and CCL17 were able to identify patient populations with significantly longer overall survival ($P < 0.007$ and $P < 0.011$, respectively), with this effect being pronounced in the +Cy arm but absent in the –Cy arm (**Fig. 5g–j**).

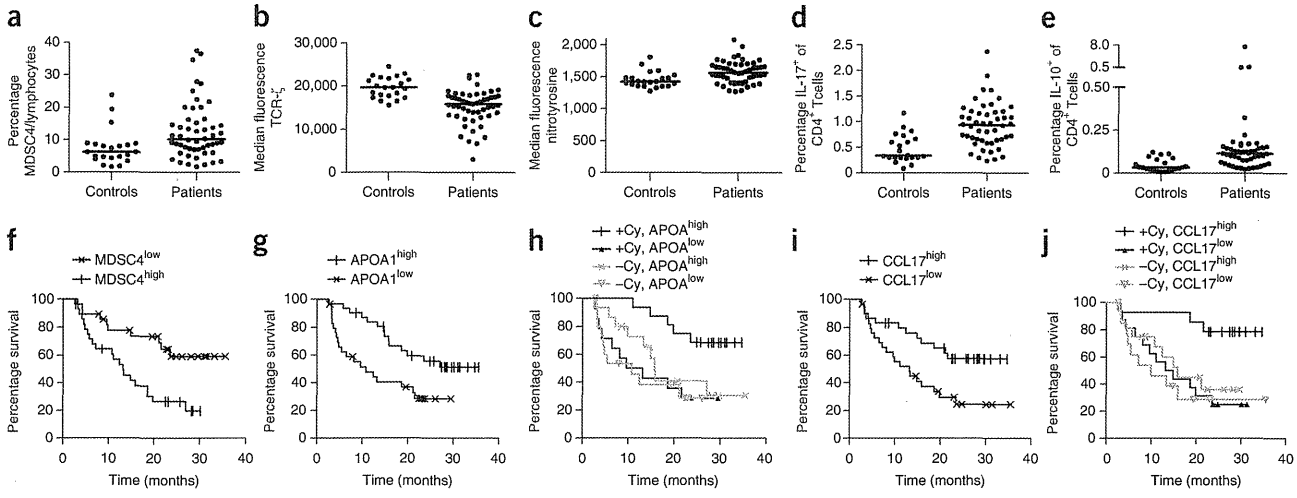

Figure 5 Analysis of pretreatment biomarkers. (**a**–**e**) Comparison of cellular biomarkers of evaluable ITT subjects aged <70 years (n = 50–53 per group) and age- and gender-matched healthy controls (n = 22). Each dot represents an individual subject, and horizontal lines represent the median values. Statistical assessments were performed using unpaired two-sided Wilcoxon tests. MDSC4, P = 0.0043 (**a**); TCR-ζ, P < 0.0001 (**b**); nitrotyrosine expression of T cells, P = 0.0038 (**c**); IL-17$^+$, P < 0.0001 (**d**); IL-10$^+$, P < 0.0001 (**e**). (**f**) Overall survival of evaluable per protocol subjects having high (n = 29) or low (n = 28) MDSC4 numbers; HR = 0.35, P = 0.0035 by log-rank test. (**g**–**j**) Overall survival in evaluable per protocol subjects having high or low concentrations of APOA1 (**g**) or CCL17 (**i**); subgroup analyses were performed with respect to cyclophosphamide pretreatment (**h**,**j**). The HR for overall survival in APOA1^{high} compared with APOA1^{low} subjects was 0.41 (P = 0.007 by log-rank test, n = 31 compared with n = 30, respectively), 0.26 in the +Cy arm (P = 0.006, n = 16 compared with n = 14) and 0.62 in the –Cy arm (P = 0.278, n = 15 compared with n = 16). The HR for overall survival in CCL17^{high} compared with CCL17^{low} subjects was 0.41 (P = 0.011 by log-rank test, n = 30 compared with n = 30, respectively), 0.19 in the +Cy arm (P = 0.003, n = 14 compared with n = 16) and 0.69 in the –Cy arm (P = 0.418, n = 16 compared with n = 14).

DISCUSSION

To the best of our knowledge, this work is the first to show that HLA-restricted peptides, selected by virtue of being naturally presented by cancer, elicit specific vaccine-induced immune responses that are associated with clinical benefit. Most therapeutic vaccine trials in cancer so far have not shown such an association, which may be explained by the lack of confirmation of natural presentation on patient-derived primary tumor tissue. In two trials testing IMA901, the breadth of the T cell response (that is, the number of different specific antigens against which T cell responses were induced by the vaccine) was significantly associated with clinical benefit, implying that the targeting of multiple antigens in immunotherapy is required for clinical efficacy. The finding that immune responses are associated with clinical benefit could be explained by therapeutic efficacy or by immune responses being merely a prognostic factor. Three observations argue in favor of the hypothesis that vaccine-induced immune responses are indeed causally related to better clinical outcome: (i) the association of immune response with clinical benefit was only observed for tumor-associated peptides and not for the unrelated nontumor HBV-derived peptide; (ii) immune responses were associated with survival only in subjects randomized to a single dose of cyclophosphamide; and (iii) the baseline characteristics were overall well matched between multipeptide immune responders, immune responders and nonresponders (**Supplementary Table 2**), and the two observed differences (age and sex) are not considered prognostic factors in advanced RCC.

Moreover, this is the first randomized trial to show that single-dose cyclophosphamide is associated with prolonged survival after tumor immunotherapy. This effect is only observed in subjects with specific immune responses to IMA901, indicating that single-dose cyclophosphamide does not have any single-agent activity (either as a cytotoxic or as a nonspecific immunomodulatory drug) but rather acts as an immunomodulator of the vaccine. Differences in baseline factors cannot explain this better outcome; if anything, subjects pretreated with cyclophosphamide tended to have a slightly worse prognosis, as exemplified by the shorter time from tumor diagnosis to randomization in this group[21,22]. The results also show that cyclophosphamide predominantly affects proliferating T_{reg} cells within the T_{reg} population. A prior report suggested that peripheral T_{reg} cells have a higher fraction of proliferating cells than do other cell subsets[34].

The survival of patients who received cytokine treatment prior to IMA901 vaccination plus cyclophosphamide (with the median overall survival not reached after 33.1 months) compared favorably with data recently published from studies with TKIs in the same setting (median overall survival of 17.8 months for sorafenib treatment compared with 15.2 months for placebo[35] and 16.4 months for sunitinib treatment[36]), whereas the overall survival of patients receiving IMA901 vaccination without cyclophosphamide (median overall survival of 15.8 months) matched these trials quite well. The baseline characteristics and risk factors of the subjects in the IMA901 phase 2 trial were generally comparable in this inter-trial comparison (**Supplementary Table 3**). Although encouraging, this observation must be interpreted with caution, as it was derived from a comparison with historical controls.

Our work also suggests that, in addition to T_{reg} cells, MDSCs may have a role in RCC outcome. Among several MDSC phenotypes described in the literature, only two populations, here termed MDSC4 and MDSC5, were shown to be negatively associated with survival in patients with RCC. Similar cellular populations have been shown to be prognostic in breast and colon cancer[37]. This observation is new for RCC and for cancer under immunotherapy. The TKI sunitinib, a standard first-line treatment in advanced RCC, has been shown to decrease the numbers of T_{reg} cells in mice[38] and patients with RCC[39], as well as MDSCs in patients with RCC[40]. Based on this

rationale, a randomized phase 3 trial combining IMA901 with single-dose cyclophosphamide and sunitinib compared with treatment with sunitinib alone was started recently[41].

The retrospective screening of a large number of serum biomarkers and their association with several outcome variables showed that two biomarkers, APOA1 and CCL17, are potentially predictive for vaccine-induced immunity and overall survival. APOA1 is the major protein component of high-density lipoprotein. Reduced concentrations of high-density lipoprotein and APOA1 are found in several types of cancer[42] and are associated with chronic inflammatory and oxidative stress, which may suppress adaptive immune responses[43]. CCL17 is a chemoattractant for several immune cells, including $CD4^+$ and $CD8^+$ T cells, in particular, skin-homing[44,45] and tumor-infiltrating T cells[46]. A major source of CCL17 is myeloid dendritic cells; constitutively as well as induced production of CCL17 has a role in dendritic cell function[47,48]. Based on these exploratory biomarker results, we hypothesize that high serum concentrations of APOA1 and CCL17 may predict immune and clinical response to IMA901.

Several aspects of the study reported here strongly suggest that therapeutic vaccinations with IMA901 induce specific immune responses that lead to clinical benefit and may be predicted by a defined pretreatment biomarker pattern. However, relatively small numbers of patients have been evaluated thus far, requiring further confirmation of clinical benefit as a prospectively defined endpoint in a large randomized clinical trial, which is currently ongoing. This randomized trial will also serve to validate the proposed predictive biomarker signature in a prospectively defined fashion.

Finally, we conclude that the rational clinical development of therapeutic cancer vaccines accompanied and guided by a comprehensive biomarker program—including T cell response monitoring, as well as monitoring of other cellular and serum biomarkers—is feasible even in multicenter trials and is valuable, provided that sample quality is tightly controlled. Such biomarkers reflect relevant mechanisms of immune induction and tolerance and assist in defining patient subpopulations with a higher prospect of response to cancer immunotherapy. These findings may have relevance for other cancer immunotherapy trials.

METHODS

Methods and any associated references are available in the online version of the paper.

Note: Supplementary information is available in the online version of the paper.

ACKNOWLEDGMENTS

We thank all investigators and patients participating in the clinical studies. Samples of healthy donors were kindly provided by D. Wernet (Institute of Clinical and Experimental Transfusion Medicine, Tübingen). The cell line K562-A2 was kindly provided by C. Britten (Tumorvakzinezentrum Mainz). This work was supported by the German 'Förderprogramm Biotechnologie Baden-Württemberg' projects 720.830-1-1/46b and 720.830-3-9, the German 'Fortüne' project 1862-0-0, the German 'Deutsche Forschungsgemeinschaft Sonderforschungsbereich 685' projects A6, C5 and C9, the German 'Bundesministerium für Bildung und Forschung' project 0315890F, the Italian 'Fondazione Cassa di Risparmio di Verona, Vicenza, Belluno e Ancona' and the Italian 'Associazione Italiana Ricerca sul Cancro' (grant 6599). We thank H. Schild for providing critical input to the manuscript and the members of the Immatics' Scientific Advisory Board and the Data Safety Monitoring Board for critical input throughout the development program.

AUTHOR CONTRIBUTIONS

S.W. designed and supervised the immunomonitoring and cellular biomarker program. T.W. designed and supervised the antigen discovery and the noncellular biomarker program. T.W. and H.S.-J. designed the composition of the drug. A.S. was the principal investigator of the IMA901 phase 1 and 2 studies and participated in the discovery phase. A.S., M.S. and P.-Y.D. treated a substantial number of patients in the phase 1 study. R.Z., A.P. and C.S. treated a substantial number of patients in the phase 2 study. W.B. was involved in the discovery phase and immunomonitoring and recruited patients in the phase 2 study. R.M., N.H. and D.M. performed and contributed essentially to the immunomonitoring. R.M. and N.H. performed and contributed essentially to the cellular biomarker program. N.H. and O.S. contributed essentially to the discovery phase and design of the clinical trials. J. Fritsche performed the bioinformatics analyses. A.M. and J. Fritsche performed and contributed essentially to the noncellular biomarker program. V.V. and C.T. supervised and performed experiments in the discovery phase. P.L. and C.F. supervised and performed the pharmaceutical development, respectively. H.P. and J.J.S. contributed essentially to the PBMC preparations for immunomonitoring. V.B., S.M., G.P. and E.D. were essentially involved in the design and data analysis of the cellular biomarker program. E.D. and T.B. performed some of the cellular biomarker experiments. H.Y., T.M., F.H., N.T., K.H. and H.T. were involved in the discovery phase. H.-G.R. and S.S. contributed essentially to the discovery phase and to the design of the overall treatment approach. H.-G.R. contributed essentially to the design of the clinical phase 1 and 2 studies. A.M.-M., H.S.-J. and J. Frisch designed the phase 1 study and planned the analysis. A.M.-M. and J. Frisch supervised the conduct and the analysis of the phase 1 study. A.K., J. Frisch and H.S.-J. designed the phase 2 study and planned the analysis. A.K. and J. Frisch supervised the conduct of the phase 2 study. A.K. and C.R. supervised the analysis of the phase 2 study. S.W., H.S.-J., T.W. and C.R. wrote the manuscript. G.P., V.B. and H.-G.R. provided critical input in the writing of the manuscript. J. Frisch and C.R. had the overall medical oversight. H.S.-J. had the overall scientific oversight. H.-G.R. provided the conceptual basis for the work presented here.

COMPETING FINANCIAL INTERESTS

The authors declare competing financial interests: details are available in the online version of the paper.

Published online at http://www.nature.com/doifinder/10.1038/nm.2883.
Reprints and permissions information is available online at http://www.nature.com/reprints/index.html.

1. Kantoff, P.W. *et al.* Overall survival analysis of a phase II randomized controlled trial of a Poxviral-based PSA-targeted immunotherapy in metastatic castration-resistant prostate cancer. *J. Clin. Oncol.* **28**, 1099–1105 (2010).
2. Schwartzentruber, D.J. *et al.* gp100 peptide vaccine and interleukin-2 in patients with advanced melanoma. *N. Engl. J. Med.* **364**, 2119–2127 (2011).
3. Schuster, S.J. *et al.* Vaccination with patient-specific tumor-derived antigen in first remission improves disease-free survival in follicular lymphoma. *J. Clin. Oncol.* **29**, 2787–2794 (2011).
4. Weinschenk, T. *et al.* Integrated functional genomics approach for the design of patient-individual antitumor vaccines. *Cancer Res.* **62**, 5818–5827 (2002).
5. Singh-Jasuja, H., Emmerich, N.P. & Rammensee, H.G. The Tubingen approach: identification, selection, and validation of tumor-associated HLA peptides for cancer therapy. *Cancer Immunol. Immunother.* **53**, 187–195 (2004).
6. Ghiringhelli, F. *et al.* Metronomic cyclophosphamide regimen selectively depletes $CD4^+CD25^+$ regulatory T cells and restores T and NK effector functions in end stage cancer patients. *Cancer Immunol. Immunother.* **56**, 641–648 (2007).
7. Motoyoshi, Y. *et al.* Different mechanisms for anti-tumor effects of low- and high-dose cyclophosphamide. *Oncol. Rep.* **16**, 141–146 (2006).
8. Ikezawa, Y. *et al.* Cyclophosphamide decreases the number, percentage and the function of $CD25^+$ $CD4^+$ regulatory T cells, which suppress induction of contact hypersensitivity. *J. Dermatol. Sci.* **39**, 105–112 (2005).
9. Lutsiak, M.E. *et al.* Inhibition of $CD4^+25^+$ T regulatory cell function implicated in enhanced immune response by low-dose cyclophosphamide. *Blood* **105**, 2862–2868 (2005).
10. Campbell, D.J. & Koch, M.A. Phenotypical and functional specialization of $FOXP3^+$ regulatory T cells. *Nat. Rev. Immunol.* **11**, 119–130 (2011).
11. Peranzoni, E. *et al.* Myeloid-derived suppressor cell heterogeneity and subset definition. *Curr. Opin. Immunol.* **22**, 238–244 (2010).
12. Gabrilovich, D.I. & Nagaraj, S. Myeloid-derived suppressor cells as regulators of the immune system. *Nat. Rev. Immunol.* **9**, 162–174 (2009).
13. Derhovanessian, E. *et al.* Pretreatment frequency of circulating $IL\text{-}17^+CD4^+$ T-cells, but not Tregs, correlates with clinical response to whole-cell vaccination in prostate cancer patients. *Int. J. Cancer* **125**, 1372–1379 (2009).
14. Zea, A.H. *et al.* Arginase-producing myeloid suppressor cells in renal cell carcinoma patients: a mechanism of tumor evasion. *Cancer Res.* **65**, 3044–3048 (2005).
15. Nagaraj, S., Schrum, A.G., Cho, H.I., Celis, E. & Gabrilovich, D.I. Mechanism of T cell tolerance induced by myeloid-derived suppressor cells. *J. Immunol.* **184**, 3106–3116 (2010).
16. Walter, S. *et al.* Cutting edge: predetermined avidity of human CD8 T cells expanded on calibrated MHC/anti-CD28–coated microspheres. *J. Immunol.* **171**, 4974–4978 (2003).

17. Rammensee, H.G., Weinschenk, T., Gouttefangeas, C. & Stevanovic, S. Towards patient-specific tumor antigen selection for vaccination. *Immunol. Rev.* **188**, 164–176 (2002).
18. Krüger, T. *et al.* Lessons to be learned from primary renal cell carcinomas: novel tumor antigens and HLA ligands for immunotherapy. *Cancer Immunol. Immunother.* **54**, 826–836 (2005).
19. Mathiassen, S., Lauemoller, S.L., Ruhwald, M., Claesson, M.H. & Buus, S. Tumor-associated antigens identified by mRNA expression profiling induce protective anti-tumor immunity. *Eur. J. Immunol.* **31**, 1239–1246 (2001).
20. Bertoletti, A. *et al.* Molecular features of the hepatitis B virus nucleocapsid T-cell epitope 18–27: interaction with HLA and T-cell receptor. *Hepatology* **26**, 1027–1034 (1997).
21. Motzer, R.J., Bacik, J., Murphy, B.A., Russo, P. & Mazumdar, M. Interferon-α as a comparative treatment for clinical trials of new therapies against advanced renal cell carcinoma. *J. Clin. Oncol.* **20**, 289–296 (2002).
22. Heng, D.Y. *et al.* Prognostic factors for overall survival in patients with metastatic renal cell carcinoma treated with vascular endothelial growth factor-targeted agents: results from a large, multicenter study. *J. Clin. Oncol.* **27**, 5794–5799 (2009).
23. Liu, W. *et al.* CD127 expression inversely correlates with FoxP3 and suppressive function of human CD4$^+$ T reg cells. *J. Exp. Med.* **203**, 1701–1711 (2006).
24. Seddiki, N. *et al.* Expression of interleukin (IL)-2 and IL-7 receptors discriminates between human regulatory and activated T cells. *J. Exp. Med.* **203**, 1693–1700 (2006).
25. Mandruzzato, S. *et al.* IL4Rα$^+$ myeloid-derived suppressor cell expansion in cancer patients. *J. Immunol.* **182**, 6562–6568 (2009).
26. Kusmartsev, S. *et al.* Reversal of myeloid cell-mediated immunosuppression in patients with metastatic renal cell carcinoma. *Clin. Cancer Res.* **14**, 8270–8278 (2008).
27. Mirza, N. *et al.* All-trans-retinoic acid improves differentiation of myeloid cells and immune response in cancer patients. *Cancer Res.* **66**, 9299–9307 (2006).
28. Filipazzi, P. *et al.* Identification of a new subset of myeloid suppressor cells in peripheral blood of melanoma patients with modulation by a granulocyte-macrophage colony-stimulation factor-based antitumor vaccine. *J. Clin. Oncol.* **25**, 2546–2553 (2007).
29. Schmielau, J. & Finn, O.J. Activated granulocytes and granulocyte-derived hydrogen peroxide are the underlying mechanism of suppression of T-cell function in advanced cancer patients. *Cancer Res.* **61**, 4756–4760 (2001).
30. Bronte, V. *et al.* Boosting antitumor responses of T lymphocytes infiltrating human prostate cancers. *J. Exp. Med.* **201**, 1257–1268 (2005).
31. Nagaraj, S. *et al.* Altered recognition of antigen is a mechanism of CD8$^+$ T cell tolerance in cancer. *Nat. Med.* **13**, 828–835 (2007).
32. Zhang, B. *et al.* The prevalence of Th17 cells in patients with gastric cancer. *Biochem. Biophys. Res. Commun.* **374**, 533–537 (2008).
33. Kryczek, I. *et al.* Cutting edge: Th17 and regulatory T cell dynamics and the regulation by IL-2 in the tumor microenvironment. *J. Immunol.* **178**, 6730–6733 (2007).
34. Tuovinen, H. *et al.* Thymic production of human FOXP3$^+$ regulatory T cells is stable but does not correlate with peripheral FOXP3 expression. *Immunol. Lett.* **117**, 146–153 (2008).
35. Escudier, B. *et al.* Sorafenib in advanced clear-cell renal-cell carcinoma. *N. Engl. J. Med.* **356**, 125–134 (2007).
36. Motzer, R.J. *et al.* Activity of SU11248, a multitargeted inhibitor of vascular endothelial growth factor receptor and platelet-derived growth factor receptor, in patients with metastatic renal cell carcinoma. *J. Clin. Oncol.* **24**, 16–24 (2006).
37. Solito, S. *et al.* A human promyelocytic-like population is responsible for the immune suppression mediated by myeloid-derived suppressor cells. *Blood* **118**, 2254–2265 (2011).
38. Hipp, M.M. *et al.* Sorafenib, but not sunitinib, affects function of dendritic cells and induction of primary immune responses. *Blood* **111**, 5610–5620 (2008).
39. Finke, J.H. *et al.* Sunitinib reverses type-1 immune suppression and decreases T-regulatory cells in renal cell carcinoma patients. *Clin. Cancer Res.* **14**, 6674–6682 (2008).
40. Ko, J.S. *et al.* Sunitinib mediates reversal of myeloid-derived suppressor cell accumulation in renal cell carcinoma patients. *Clin. Cancer Res.* **15**, 2148–2157 (2009).
41. Rini, B.I. *et al.* IMA901 Multipeptide Vaccine Randomized International Phase III Trial (IMPRINT): a randomized, controlled study investigating IMA901 multipeptide cancer vaccine in patients receiving sunitinib as first-line therapy for advanced/metastatic RCC. *J. Clin. Oncol.* **29** (suppl.15), abstr. TPS183 (2011).
42. Muntoni, S. *et al.* Serum lipoproteins and cancer. *Nutr. Metab. Cardiovasc. Dis.* **19**, 218–225 (2009).
43. Burger, D. & Dayer, J.M. High-density lipoprotein-associated apolipoprotein A-I: the missing link between infection and chronic inflammation? *Autoimmun. Rev.* **1**, 111–117 (2002).
44. Andrew, D.P. *et al.* C–C chemokine receptor 4 expression defines a major subset of circulating nonintestinal memory T cells of both Th1 and Th2 potential. *J. Immunol.* **166**, 103–111 (2001).
45. Bromley, S.K., Mempel, T.R. & Luster, A.D. Orchestrating the orchestrators: chemokines in control of T cell traffic. *Nat. Immunol.* **9**, 970–980 (2008).
46. Kanagawa, N. *et al.* CC-chemokine ligand 17 gene therapy induces tumor regression through augmentation of tumor-infiltrating immune cells in a murine model of preexisting CT26 colon carcinoma. *Int. J. Cancer* **121**, 2013–2022 (2007).
47. Real, E. *et al.* Immature dendritic cells (DCs) use chemokines and intercellular adhesion molecule (ICAM)-1, but not DC-specific ICAM-3–grabbing nonintegrin, to stimulate CD4$^+$ T cells in the absence of exogenous antigen. *J. Immunol.* **173**, 50–60 (2004).
48. Semmling, V. *et al.* Alternative cross-priming through CCL17–CCR4-mediated attraction of CTLs toward NKT cell-licensed DCs. *Nat. Immunol.* **11**, 313–320 (2010).
49. Schmidt, S.M. *et al.* Induction of adipophilin-specific cytotoxic T lymphocytes using a novel HLA-A2–binding peptide that mediates tumor cell lysis. *Cancer Res.* **64**, 1164–1170 (2004).
50. Sadovnikova, E., Jopling, L.A., Soo, K.S. & Stauss, H.J. Generation of human tumor-reactive cytotoxic T cells against peptides presented by non-self HLA class I molecules. *Eur. J. Immunol.* **28**, 193–200 (1998).
51. Schag, K. *et al.* Identification of C-met oncogene as a broadly expressed tumor-associated antigen recognized by cytotoxic T-lymphocytes. *Clin. Cancer Res.* **10**, 3658–3666 (2004).
52. Brossart, P. *et al.* Identification of HLA-A2–restricted T-cell epitopes derived from the MUC1 tumor antigen for broadly applicable vaccine therapies. *Blood* **93**, 4309–4317 (1999).
53. Brossart, P. *et al.* Induction of cytotoxic T-lymphocyte responses *in vivo* after vaccinations with peptide-pulsed dendritic cells. *Blood* **96**, 3102–3108 (2000).
54. Brossart, P. *et al.* The epithelial tumor antigen MUC1 is expressed in hematological malignancies and is recognized by MUC1-specific cytotoxic T-lymphocytes. *Cancer Res.* **61**, 6846–6850 (2001).
55. Wierecky, J. *et al.* Immunologic and clinical responses after vaccinations with peptide-pulsed dendritic cells in metastatic renal cancer patients. *Cancer Res.* **66**, 5910–5918 (2006).
56. Boss, C.N. *et al.* Identification and characterization of T-cell epitopes deduced from RGS5, a novel broadly expressed tumor antigen. *Clin. Cancer Res.* **13**, 3347–3355 (2007).
57. Dengjel, J. *et al.* Unexpected abundance of HLA class II presented peptides in primary renal cell carcinomas. *Clin. Cancer Res.* **12**, 4163–4170 (2006).
58. Ruppert, J. *et al.* Prominent role of secondary anchor residues in peptide binding to HLA-A2.1 molecules. *Cell* **74**, 929–937 (1993).

ONLINE METHODS

Phase 1 study design. Between 2005 and 2006, we conducted a multicenter, single-arm, open-label first-in-man study at six study sites in three European countries in accordance with the Declaration of Helsinki, current International Conference on Harmonisation of Technical Requirements for Registration of Pharmaceuticals for Human Use (ICH) guidelines and all applicable regulatory and ethical requirements. All subjects provided written informed consent before study-related procedures were performed. Subjects with histologically confirmed RCC of American Joint Committee on Cancer Stages 3 and 4 were enrolled.

Each of the vaccinations consisted of an intradermal (i.d.) injection of GM-CSF (75 μg) followed within 15–30 min by an i.d. injection of IMA901 (413 μg of each peptide). The vaccine therapy was a monotherapy, meaning that no other antitumor therapies were concomitantly administered during the study course. Of the 28 HLA-A*02–positive patients, 27 patients received eight vaccinations and 1 patient was prematurely withdrawn and received only one vaccination.

The primary endpoint was safety and tolerability. Main secondary endpoints were immunogenicity and evidence of antitumor activity.

Phase 2 study design and treatment schedule. Between 2007 and 2009, we conducted a multicenter, randomized, open-label phase 2 study in accordance with the Declaration of Helsinki, current ICH guidelines and all applicable regulatory and ethical requirements. All subjects provided written informed consent before study-related procedures were performed. Subjects were recruited by 23 centers across ten European countries. Subjects were randomized to receive or not receive one single infusion of cyclophosphamide (300 mg m^{-2}) 3 d before the first vaccination with IMA901 plus GM-CSF. The phase 2 injection doses of IMA901 per peptide and GM-CSF were identical to the phase 1 study, however formulation in the phase 2 study excluded the marker peptide HBV-001. Stratification factors included risk group (Memorial Sloan-Kettering Cancer Center (MSKCC) three-item score, with only favorable and intermediate risk patients being eligible) and previous treatment (cytokine or TKI). Subjects had to have measurable lesions to be eligible for the trial; other relevant inclusion criteria were documented tumor progression during or after previous systemic therapy and Karnofsky performance status ≥80%. Subjects with brain metastases, relevant autoimmune diseases, other malignancies or major abnormalities of hematology, liver and renal function tests were excluded. No treatment with either anticancer agents or immunosuppressants was allowed within 4 weeks before entering the trial. Subjects in both treatment arms were to receive seven vaccinations in the first 5 weeks of treatment (induction period) followed by ten further vaccinations at 3 week intervals for up to 30 weeks (maintenance period). Subjects were prospectively defined as per protocol if they received at least six vaccinations with IMA901 and GM-CSF.

The primary endpoint was DCR after 6 months. Main secondary endpoints were PFS, overall survival, immunogenicity and safety.

Clinical assessment criteria. The safety of study treatment was assessed in both trials based on the occurrence of adverse events, which were categorized and graded according to National Cancer Institute Common Toxicity Criteria (NCI-CTC).

Evidence of antitumor activity was obtained in terms of tumor size of target lesions and evaluation of nontarget lesions at baseline (that is, during the screening period) and at the respective follow-up visits as per RECIST 1.0.

In the phase 1 study, tumor follow-up assessment was compared with baseline. In the phase 2 study, tumor assessments were performed every 6 weeks (except for the first assessment, which occurred 8.5 weeks after cyclophosphamide administration). Tumor images were centrally reviewed by independent radiologists and one oncologist (Perceptive Informatics Inc., Berlin, Germany). Further follow up to collect survival data was conducted at 3-month intervals. The phase 2 trial is registered and has ClinicalTrials.gov identifier NCT01265901. The ongoing phase 3 trial, which is mentioned in the Discussion section, has the ClinicalTrials.gov identifier NCT00523159.

Immunomonitoring and biomarker analysis. PBMCs were isolated from subjects within 8 h of venipuncture using fully standardized procedures, cryopreserved and shipped for central laboratory analysis. We detected T cell responses to individual HLA-A*02–binding peptides by performing HLA multimer staining and interferon γ (IFN-γ) enzyme-linked immunospot (ELISPOT) after antigen stimulation and 12 d of *in vitro* culture. We assessed the numbers of T_{reg} cells and MDSCs and the expressions of TCR-ζ and nitrotyrosine on T cells by *ex vivo* multicolor flow cytometric analyses. We performed assessment of T_H subset numbers by intracellular cytokine staining after a 5 h stimulation with phorbol 12-myristate 13-acetate (PMA) and ionomycin. We measured serum biomarkers using multiplex technologies, mass spectrometry and ELISA.

Statistical analyses. In the phase 1 study, we analyzed the association of immune responses with DCR using a two-sided χ^2 test and the association of T_{reg} cells with immune responses retrospectively using a two-sided Wilcoxon test.

In the phase 2 study, we performed prospectively defined binary survival comparisons of study subgroups using log-rank tests and deduced survival rates from Kaplan-Meyer plots. We indicated 95% confidence intervals in the text. In the case of multiple immune response groups, the log-rank test for trend was used testing the null hypothesis that there is no linear trend between increasing numbers of immune responses and median survival.

We assessed the decrease of absolute T_{reg} cell numbers from VC to V1 with a prospectively defined paired two-sided Wilcoxon test and used the same test in the *post-hoc* analysis of Ki-67^+ cells within T_{reg} cells.

In further *post-hoc* analyses, we used an unpaired two-sided Wilcoxon test to compare the number of MDSCs, T_H subset frequencies and expressions of age- and gender-matched patients and healthy controls. We performed correlation analyses among cellular biomarkers *post hoc* using a Pearson product-moment correlation.

We performed all serum biomarker analyses retrospectively: an unpaired Welch's *t* test was used for association of serum biomarkers with T cell responses. We assessed the association of continuous biomarker parameters with overall survival in a univariate Cox proportional hazards model. To use continuous parameters as classifiers distinguishing between subjects with more and less survival benefit, we used the median concentrations derived from the per protocol population as a cutoff. The log-rank test was performed for binary survival comparisons.

We performed statistical analyses using R (GNU) programming language using the package 'survival', GraphPad Prism 4 (GraphPad Software) and Statgraphics Centurion (Statpoint Technologies).

Identification and gene expression analysis of HLA-restricted peptides. After approval by the relevant Institutional Review Boards at the University of Tübingen and Kyoto Prefectural University of Medicine and informed consents given by the patients, HLA peptide pools from shock-frozen tissue samples were obtained by immune precipitation from solid tissues using the HLA-A*02–specific antibody BB7.2 (ref. 59) for HLA-A*02^+ patients (BB7.2 was kindly provided by H.-G.R., antibody amounts used for precipitation were adopted to the weight of each tissue and ranged from 10–25 mg). Peptides were sequenced using a quadrupole time of flight (Q-TOF) mass spectrometer, as described elsewhere[18], or separated using a nanoAcquity UPLC system (Waters, Eschborn, Germany) and analyzed in an LTQ-Orbitrap mass spectrometer (Thermo Fisher Scientific, Bremen, Germany). All selected sequences were verified by comparison with the spectra of synthetic peptides (data not shown). Gene expression analysis was performed using high-density oligonucleotide microarrays, as previously described[18].

RCC samples included samples from European and Japanese patients and had to fulfill standardized quality criteria to be evaluable. No relevant differences in mRNA expression or peptide presentation of the TUMAPs contained in IMA901 between the European and Japanese patients were observed. IMA901 TUMAPs were found on HLA-A*0201^+ as well as on HLA-A*0206^+ tumor tissues (data not shown).

***In vitro* validation of TUMAP immunogenicity.** *In vitro* T cell priming using artificial antigen-presenting cells loaded with high-density HLA-peptide complexes and antibodies to CD28 was performed as described previously[16].

Peptide vaccine preparation. All individual peptides and the final multipeptide vaccine IMA901 have been manufactured in compliance with good manufacturing

doi:10.1038/nm.2883

practice and in accordance to predefined release specifications. Peptides were manufactured with purities ≥95.0% (Bachem AG, Bubendorf, Switzerland) with a free N terminus, free C terminus and acetate or hydrochloride as a counter ion using standard solid-phase procedures. IMA901 was formulated (Rentschler Biotechnologie GmbH, Laupheim, Germany), labeled, packaged and distributed to clinical sites (Penn Pharmaceutical Services, Tredegar, UK). IMA901 for clinical phase 1 was formulated by mixing solutions of the 11 peptides, as listed in **Table 1**, lyophilised without the addition of excipients and resolubized with 4.2% sodium bicarbonate buffer (Braun AG, Melsungen, Germany). For clinical phase 2, the formulation of IMA901 comprised all peptides also used for phase 1, with the exception of HBV-001, with added mannitol (Merck KGaA, Darmstadt, Germany) and poloxamer 188 (Lutrol F68) (BASF Chemtrade GmbH, Burgbernheim, Germany) as excipients. Addition of these excipients did not alter the immunological properties of the vaccine, as shown in preclinical vaccination studies. Briefly, C57BL/6 mice were immunized with the ovalbumin-derived peptide SIINFEKL and CpG deoxyoligonucleotide as an immunomodulator in 4.2% bicarbonate buffer with or without poloxamer 188 and mannitol added at concentrations identical to those in the later formulation of IMA901 for the phase 2 trial. Mice were killed 9 d after immunization, and the frequency of peptide-specific $CD8^+$ T cells was estimated. There was no difference in immune responses between the groups with and without the excipients (data not shown).

Quality control of the identity of the specified parameters, the content of active ingredients, the uniformity of content, the purity and the product-related impurities of the formulated product included the implementation of a validated analytical HPLC method, which was able to separate each individual peptide. Using this method, stability studies of the lyophilized product did not show any substantial decrease in peptide content or in peptide purity (product-related impurities) when the vaccine was stored at 25 °C (60% relative humidity), 5 °C and −20 °C for up to 36 months (data not shown). In accordance with the stability data obtained after reconstitution, the peptide vaccine IMA901 had to be used within 1 h after reconstitution on clinical sites.

Immunomodulators. The immunomodulators GM-CSF (sargramostim, Leukine; Genzyme, Seattle, USA) and cyclophosphamide (Endoxan; Baxter, UK) were purchased as good manufacturing practice grade lyophilisates and administered i.d. or intravenously, respectively, according to the manufacturer's instructions.

PBMC sample acquisition. PBMCs were isolated from 50 ml (phase 1) or 100 ml (phase 2) sodium heparine blood within 8 h of venipuncture using a standard Ficoll-Hypaque density gradient procedure and were cryopreserved in serum-free medium. At sites where this was feasible, cells were stored in the gas phase of liquid nitrogen before shipment; otherwise cells were directly shipped within 7 d of storage at −80 °C. After shipment to the central laboratory on dry ice, frozen cells were stored in the gas phase of liquid nitrogen until use. All media and reagents were standardized, tested and supplied centrally as kits. All crucial steps of PBMC sample acquisition were performed according to standard operating procedures by specifically trained personnel. Laboratories isolating PBMCs had to pass a documented qualification procedure, including the successful performance of test runs.

Discussion of the choice of assay for detection of T cell responses. The T cell assays performed routinely for patients in the IMA901 phase 1 and phase 2 studies were '*in vitro* stimulation assays', which involve a 12-d cell culture after peptide pulsing. This contrasts to the quantification of T cells '*ex vivo*' without prior cell culture but does not constitute '*in vitro* priming' of naive T cells, for which professional antigen-presenting cells have to be used *in vitro* (see **Fig. 1d** for an example of *in vitro* priming).

We justify this choice based on a number of observations and further assumptions. (i) For a subset of six patients of the IMA901 phase 1 study, for whom *ex vivo* IFN-γ ELISPOT assays were performed, no patients showed *ex vivo*–measurable vaccine-induced immune responses, whereas four showed a measurable IFN-γ ELISPOT response after *in vitro* stimulation. (ii) The amplification factor of the *in vitro* stimulation assay was ~100× based on direct comparisons (*ex vivo* compared with *in vitro* stimulated) of virus-specific T cell responses ($n = 33$), as well as strong patient vaccine-induced responses ($n = 3$; data not shown). Based on this observation, it can be assumed that the majority of the observed T cell responses of IMA901 phase 1 and phase 2 patients were well below the detection threshold of current *ex vivo* multimer assays (~0.01%). (iii) The empirical threshold for detection of a vaccine-induced response was set to a conservative value (4× above baseline), as the *in vitro* culture is expected to be associated with a resulting lower precision as compared with an *ex vivo* assay. (iv) In several reported immunotherapy studies[60–64], *ex vivo* detectable, vaccine-induced T cell responses in patients with melanoma were readily detected. It is worth noting that in these studies, altered ligands or the HLA-A*02-restricted Melan-A peptide were almost exclusively used. It is expected that for altered, nonself antigens, higher precursor frequencies of naive T cells as compared with self antigens can be found. For the particular Melan-A peptide used, an abnormally high precursor frequency of naive T cells has been shown[65]. However, the biological relevance of altered ligands as vaccine targets is subject to debate[66], as high-frequency T cells specific to the altered peptide may not crossreact to the unaltered peptide that is presented by the tumor.

We conclude that for the detection of vaccine-induced responses to self antigens in patients with cancer, *in vitro* stimulation assays are the current technical state of the art, as such responses are often below the detection limit of current *ex vivo* assays. The low-frequency responses in the peripheral blood that are detected by the *in vitro* (but missed by the *ex vivo*) assay may be biologically relevant, as indicated by the phase 1 and 2 IMA901 studies and other studies. This biological relevance of low-frequency responses in the blood may be explained by higher T cell frequencies in other compartments (for example, lymph nodes, bone marrow or tumor sites) or association with epitope spreading to other targets.

Assessment of T cell responses. Vaccine-induced T cell responses to HLA-A*02 binding peptides were identified by HLA multimer staining or IFN-γ ELISPOT after one 12-d *in vitro* stimulation of samples of patients with peptides from single or pooled blood drawings, as specified below. For all patients, both assays were performed, and patients had to be evaluable for at least one assay for each peptide at each visit during which immunomonitoring was scheduled. Because of the technical limitations of the assays, no readout was available for the single HLA-DR–associated peptide. In both assays, time point pools were used from the limited amount of blood to derive a full dataset for all HLA class I peptides contained in IMA901 plus the controls (phase 1: VC/V1 (pooled), V4/V5, V6/V7, V8/FU; phase 2: VC/V1, V5, V6, V7). Additionally, PBMC samples for each single time point were analyzed by multimer staining in a subset of nine patients with 13 detected responses in the phase 1 study to investigate kinetics of T cell responses.

For each analysis time point, approximately 1.2×10^7 thawed PBMCs in a concentration of 2.5×10^6 to 5.4×10^6 ml^{-1} were incubated in X-Vivo 15 plus 2 mM L-glutamine (Lonza, Verviers, Belgium or Life Technologies, Darmstadt, Germany) containing all IMA901 class I peptides used for immunization (10 μg ml^{-1} per peptide) for 2 h at 37 °C, 5% CO_2 and 95% humidity. Cells were pelleted, resuspended in X-Vivo 15 supplemented with 10% heat-inactivated human AB Serum (C.C. Pro, Neustadt/W., Germany or PAN, Aidenbach, Germany), 2 mM L-glutamine, 100 U ml^{-1} penicillin, 100 μg ml^{-1} streptomycin (Lonza) and 20 U ml^{-1} IL-2 (Novartis, Munich, Germany) and cultured for 12 d. Half of the medium was replaced every 2–3 d.

ELISPOT assay. The IFN-γ ELISPOT assessment was performed using the ELISPOT-IFN-γ Set and the AEC Substrate Reagent Set (both by Becton Dickinson, Heidelberg, Germany), according to the manufacturer's protocol. For stimulations, PBMCs were harvested on day 13, washed in CTL-Wash (CTL, Cleveland, USA), supplemented with 2 mM L-glutamine and re-stimulated for readout in CTL-Test (CTL) supplemented with 2 mM L-glutamine. For each peptide assessment, 75,000 effector cells per well were incubated with 100,000 untreated K562-A2 cells[67] (phase 1) or 75,000 K562-A2 cells[67] pretreated with 100 U ml^{-1} human IFN-γ (Boehringer Ingelheim, Ingelheim, Germany) (phase 2) and 10 μg ml^{-1} of peptide for 20–24 h at 37 °C and 5% CO_2. Readout was performed on a Series 3B ELISPOT Reader (CTL). Each sample was tested in triplicate, and the presence of vaccine-induced response was determined according to objective criteria based on suggestions by the international Association for Cancer Immunotherapy (CIMT) Immunoguiding

Program (CIP) and others[68,69]. Briefly, the mean spot number for a given peptide had to be at least twofold over the mean background spot number, and the difference of the triplicates had to pass the Student's *t* test ($P < 0.05$, two sided). Furthermore, the ratio of peptide to negative control mean for a given post-vaccination time point had to be at least twofold over the corresponding ratio before vaccination.

HLA multimer assay. Dual HLA multimer assessment was performed as shown previously[70] with minor modifications. Briefly, PBMCs were harvested on day 13 and approximately 0.5×10^6 to 1×10^6 PBMCs per staining were treated first with HLA-A*0201 multimer phycoerythrin and HLA-A*0201 multimer allophycocyanin (individually at 5 μg ml^{-1} HLA concentration plus all multimers in one pool each at 1 μg ml^{-1}) (phase 1) or LIVE/DEAD fixable Aqua dead cell stain kit (Life Technologies) followed by multimers (phase 2) and then by antibodies to CD8 (SK1, 1:20, BD) plus antibodies to CD3 (UCHT1, 1:40, BD). Cells were fixed and analyzed on a FACSCalibur (phase 1, BD) or LSRII SORP cytometer (phase 2, BD). FCSExpress (DeNovo Software, Los Angeles, USA) or FlowJo (Tree Star, Ashland, USA) was used to enumerate single multimer-positive cells among $CD8^+CD3^+$ lymphocytes. Detailed gating and representative dot plots are shown in **Supplementary Figures 2** and **3**. The presence of a vaccine-induced response was determined according to objective criteria based on suggestions by the international Association for Cancer Immunotherapy (CIMT) Immunoguiding Program (CIP) and others[68,69]. Briefly, frequencies of multimer-positive cells must have been at least fourfold over the corresponding frequency before vaccination. Furthermore, in dot plots, multimer-positive cell populations must have been clustered and discrete from multimer-negative cells. In phase 2, this was determined by the evaluation of blinded data by a jury consisting of five members. The jury members had to evaluate whether the multimer-stained cell population was clearly clustered and discrete. Each jury member could attribute up to two points, and a vaccine-induced immune response was only identified if at least nine points were given. Cells must have been specifically stained with one single HLA multimer to exclude particles nonspecifically binding to all HLA multimers.

Assessment of T_{reg} cells. PBMC samples were thawed in the presence of 0.5 U ml^{-1} Benzonase (Merck, Darmstadt, Germany).

In phase 1, quantification of T_{reg} cells was performed according to the manufacturers' protocol of the FOXP3 (PCH101, 1:5) staining set and antibody to CD4 (L3T4, 1:4) (both obtained from eBioscience, San Diego, USA) and CD45 (2D1, 1:4, BD). The sample analysis was performed on a FACSCalibur cytometer, and data analysis was performed using FCSExpress. All T_{reg} cell measurements were performed in one single assay, and quantification was based on an automatically adjusted percentile quadrant (99.7% FOXP3 percentile on $CD4^-CD45^+$ lymphocytes). The results using CD4, FOXP3 and CD45 were later confirmed with a selected subset of patient samples by a four-color cytometric analysis that included CD25 (BC96, 1:5; data not shown).

In phase 2, quantification of T_{reg} cells among PBMCs was performed by the LIVE/DEAD fixable Aqua dead cell stain kit followed by surface staining for CD45 (F10-89-4, 1:00, AbD Serotec, Düsseldorf, Germany), CD4 (S3.5, 1:600) and CD8 (3B5, 1:400, both Life Technologies), CD3 (SK7, 1:80), CD25 (M-A251, 1:5), CD127 (human IL-7R–M21, 1:20) and CD45RA (L48, 1:240, all from BD). Erythrocytes were lysed with Pharm-Lyse-Solution (BD), and cells were fixed and permeabilized (FOXP3 staining buffer set, eBiosciences) followed by intracellular staining for FOXP3 (206D, 1:8, Biolegend, Fell, Germany) and Ki-67 (B56, 1:10, BD). Fluorochromes were carefully chosen to optimize the signal-to-noise ratio on the instrument platform according to criteria described before[71]. After fixation with 1% formaldehyde, cells were analyzed on a BD LSRII SORP cytometer, and data analysis was performed using FlowJo (TreeStar). Identical gates (**Supplementary Fig. 4**) were established for all samples and in all assays with the help of fluorescence minus one (FMO) and isotype controls that clearly identified the outlines of the populations. Samples were set evaluable if at least 75,000 live $CD45^+$ lymphocytes were counted. To assess T_{reg} cell kinetics data for individual patients, a total of seven assays were performed, and the data were pooled. To control the interassay variability of the T_{reg} cell assays, ten additional unique healthy donor control samples were thawed and stained in each experiment. Data bridging between assays was ensured by assay standardization, calibrated instrument settings, standardized data evaluation procedures and comparison with internal PBMC controls.

To assess the precision of the assay, several analyses were performed. First, the evaluation of the ten unique control samples that were repeated in each of the phase 2 T_{reg} cells assays described above resulted in a mean interassay coefficient of variation (CV) of 13%. In an independent validation study, testing a panel of 13 different healthy donor samples resulted in a mean interassay CV of 7.1%. The large majority (58 of 60) of patient kinetics were evaluated from assays containing all time points of a patient, and, therefore, the (generally lower) intra-assay CV should be applied for these analyses. From the analysis of replicate samples within one assay, we determined in one study an intra-assay CV of 9.6% and in another study an intra-assay CV of 4.4%.

Absolute T_{reg} cell frequencies were calculated by multiplying relative T_{reg} cell numbers within $CD45^+$ lymphocytes measured by flow cytometry with absolute lymphocyte counts from hematology. Hematology was not performed at VC for the –Cy arm. Therefore, absolute T_{reg} cell numbers for VC in the –Cy arm were calculated with lymphocyte counts from V1 (3 d after VC).

Matched comparisons of cellular biomarkers between patients and healthy donors. PBMCs of healthy blood bank donors (Institute of Clinical and Experimental Transfusion Medicine, Tübingen) were obtained after informed consent from all subjects and approval of the protocol by the local Institutional Review Board at the University of Tübingen. For comparison of pretreatment concentrations with healthy donors, ITT patients below the age of 70 were selected. The resulting groups of patients and controls were balanced with respect to age, gender and cytomegalovirus seropositivity.

Assessment of MDSC frequencies, TCR-ζ and nitrotyrosine expression. PBMC samples were thawed in the presence of 0.5 U ml^{-1} Benzonase (Merck).

For the assessment of MDSCs, cells were first stained with the LIVE/DEAD fixable Aqua dead cell stain kit. Cells were then blocked with human IgG (AbD Serotec) to reduce subsequent Fc-mediated binding. Cells were then surface stained with antibodies to CD45 (HI30, 1:100, Life Technologies), antibodies to CD15 (MMA, 1:80), CD11b (ICRF44, 1:640), CD124 (human IL-4R–M57, 1:10), CD14 (MφP9, 1:60), CD33 (P.67.6, 1:320), Lineage marker (consisting of CD3 (UCHT1, 1:40), CD14 (M5E2, 1:40) and CD19 (HIB19, 1:320) and CD56 (NCAM16.2, 1:80, all by BD)). Erythrocyte lysis and fixation was performed with FACS lysing solution (BD).

For the assessment of TCR-ζ and nitrotyrosine, cells were first stained with the LIVE/DEAD fixable Aqua dead cell stain kit. Cells were then surface stained with antibodies to CD4 (S3.5, 1:300), CD8 (3B5, 1:400, both Life Technologies), CD45 (F10-89-4, 1:100, AbD) and CD3 (SK7, 1:160, BD). Stained cells were lysed for erythrocytes (Pharm-Lyse-Solution, BD), permeabilized and fixed (eBioscience). After intracellular staining with antibodies to CD3-ζ (1A6, 1:20, Santa Cruz Biotechnology, Santa Cruz, USA) and antibodies to nitrotyrosine (6B10.2, 1:50, Merck Millipore, Schwalbach, Germany), cells were again fixed with formaldehyde (Fluka, Munich, Germany).

Fluorochromes of the multicolor assays were carefully chosen to optimize the signal-to-noise ratio on the instrument platform according to criteria described before[71]. Measurement was performed on an LSR II SORP instrument (BD). All samples were analyzed in one experiment for each assay type. The data analysis was performed with FlowJo (TreeStar). Identical gates were used for all samples (**Supplementary Fig. 5**). Samples were set evaluable if at least 75,000 live $CD45^+$ lymphocytes were counted.

Assessment of T_H cell subsets. After thawing, PBMCs were stimulated for 5 h with 50 ng ml^{-1} PMA (Sigma Aldrich, Munich, Germany) and 750 ng ml^{-1} ionomycin (Merck) at 37 °C. After treatment with GAMUNEX (Bayer, Leverkusen, Germany) and ethidium monoazide (Life Technologies) for 10 min on ice, cells were stained for CD3 (UCHT1, 1:250, Life Technologies), CD4 (RPA-T4, 1:250, BioLegend), CD8 (SK1, 1:25), CCR4 (1G1, 1:15) and CCR6 (11A9, 1:25, all BD). Cells were then permeabilized with a Cytofix/Cytoperm kit (BD) and stained with antibodies to IL-17 (eBio64DEC17, 1:5, eBiosciences), tumor necrosis factor α (TNF-α) (cA2, 1:10), IL-10 (B-T10, 1:6, Miltenyi Biotech, Bergisch Gladbach, Germany) and IFN-γ (B27, 1:250, BioLegend). Cells were analyzed immediately on an LSR II cytometer with FACSDiva software

doi:10.1038/nm.2883

(BD Biosciences). In all experiments at least 1×10^6 cells were measured. One control donor was always included in each experiment. Flow cytometry staining and data analysis were performed on blinded patient samples.

Serum biomarker sample collection. All serum samples were collected at visit VC. Samples were taken using a serum/gel-VACUTAINER 5 ml (BD), inverted and incubated for a minimum of 30 min. Tubes were centrifuged for 15 min at ≥1,200 *g*, and serum (approximately 2 ml) was transferred into a NUNC cryotube (3.6 ml). Cryotubes were stored immediately at or below −20 °C until measurement.

Serum biomarker analyses. More than 300 serum analytes (cytokines, chemokines, other proteins and metabolites) were measured using various multiplex technologies, mass spectrometry and ELISA.

APOA1 was measured by Rules Based Medicine (RBM, Austin, TX) as part of a multiplex assay using luminex technology (Human MAP v1.6). CCL17 measurement was part of a tenplex cytokine panel provided by Millipore, and the assay was performed in the Naturwissenschaftliches und Medizinisches Institut (NMI) in Reutlingen, Germany.

59. Parham, P. & Brodsky, F.M. Partial purification and some properties of BB7.2. A cytotoxic monoclonal antibody with specificity for HLA-A2 and a variant of HLA-A28. *Hum. Immunol.* **3**, 277–299 (1981).
60. Kirkwood, J.M. *et al.* Immunogenicity and antitumor effects of vaccination with peptide vaccine+/–granulocyte-monocyte colony-stimulating factor and/or IFN-α2b in advanced metastatic melanoma: Eastern Cooperative Oncology Group Phase II Trial E1696. *Clin. Cancer Res.* **15**, 1443–1451 (2009).
61. Baumgaertner, P. *et al. Ex vivo* detectable human CD8 T-cell responses to cancer-testis antigens. *Cancer Res.* **66**, 1912–1916 (2006).
62. Liénard, D. *et al. Ex vivo* detectable activation of Melan-A–specific T cells correlating with inflammatory skin reactions in melanoma patients vaccinated with peptides in IFA. *Cancer Immun.* **4**, 4 (2004).
63. Speiser, D.E. *et al.* Rapid and strong human CD8$^+$ T cell responses to vaccination with peptide, IFA, and CpG oligodeoxynucleotide 7909. *J. Clin. Invest.* **115**, 739–746 (2005).
64. Walker, E.B. *et al.* gp100(209–2M) peptide immunization of human lymphocyte antigen-A2$^+$ stage I–III melanoma patients induces significant increase in antigen-specific effector and long-term memory CD8$^+$ T cells. *Clin. Cancer Res.* **10**, 668–680 (2004).
65. Pittet, M.J. *et al.* High frequencies of naive Melan-A/MART-1–specific CD8$^+$ T cells in a large proportion of human histocompatibility leukocyte antigen (HLA)-A2 individuals. *J. Exp. Med.* **190**, 705–715 (1999).
66. Speiser, D.E. *et al.* Unmodified self antigen triggers human CD8 T cells with stronger tumor reactivity than altered antigen. *Proc. Natl. Acad. Sci. USA* **105**, 3849–3854 (2008).
67. Britten, C.M. *et al.* The use of HLA-A*0201–transfected K562 as standard antigen-presenting cells for CD8$^+$ T lymphocytes in IFN-γ ELISPOT assays. *J. Immunol. Methods* **259**, 95–110 (2002).
68. Britten, C.M. *et al.* The CIMT-monitoring panel: a two-step approach to harmonize the enumeration of antigen-specific CD8$^+$ T lymphocytes by structural and functional assays. *Cancer Immunol. Immunother.* **57**, 289–302 (2008).
69. Chianese-Bullock, K.A. *et al.* MAGE-A1-, MAGE-A10-, and gp100-derived peptides are immunogenic when combined with granulocyte-macrophage colony-stimulating factor and montanide ISA-51 adjuvant and administered as part of a multipeptide vaccine for melanoma. *J. Immunol.* **174**, 3080–3086 (2005).
70. Walter, S. *et al.* High frequencies of functionally impaired cytokeratin 18-specific CD8$^+$ T cells in healthy HLA-A2$^+$ donors. *Eur. J. Immunol.* **35**, 2876–2885 (2005).
71. Mahnke, Y.D. & Roederer, M. Optimizing a multicolor immunophenotyping assay. *Clin. Lab. Med.* **27**, 469–85 (2007).